# ABIOTIC NITRATE REDUCTION BY REDOX ACTIVATED IRON-BEARING SMECTITES

BY

ZACHARY B. DAY

THESIS

Submitted in partial fulfillment of the requirements
for the degree of Master of Science in Natural Resources and Environmental Sciences
in the Graduate College of the
University of Illinois at Urbana-Champaign, 2010

Urbana, Illinois

Master's Committee:

Professor Emeritus Joseph W. Stucki, Chair
Professor Richard L. Mulvaney
Professor Gregory S. Girolami

## ABSTRACT

Nitrate is a contaminant of interest in soils and water. It has been linked to chronic human illness and a variety of environmental problems, including hypoxia in coastal waters. Previous work has shown that nitrate is naturally removed from soils below the redox interface of the soil profile. A lack of denitrifying bacteria in the studied profiles points to an abiotic source of nitrate reduction that likely involves mineral phases containing iron. The ability of reduced, iron-bearing clay minerals to in turn reduce nitrate was investigated using SWa-1 chemically reduced by sodium dithionite. Analysis of ferrous and total iron concentrations in the reduced clay was performed with a colorimetric 1,10-phenanthroline method before and after reaction with a dilute nitrate solution to observe reoxidation of the clay structure. This was paired with chemiluminescent nitrogen analysis of the dilute nitrate solution to determine that not only are these reduced clay samples capable of reducing nitrate, but also that the extent of reduction plays a key role in the reductive capacity. A strikingly linear response was found between the amount of ferrous iron present in the clay structure and the amount of nitrate that was removed from the system. An additional approach for monitoring such reactions as they occur with an oxygen-free flow reactor connected to a UV-Vis spectrometer was also evaluated. These flow reactor experiments sought to investigate the differences in nitrate reductive capacity between the chemically reduced clay, bacteria reduced clay, and clay reduced in the presence of zero-valent iron. This method proved inferior to the more rigorous approach of chemically analyzing iron and nitrate concentrations. Experiments were also performed to test the effects of an electron shuttle by addition of anthraquinone-2,6-disulfonate to samples of bacteria and dithionite reduced clays using the phenanthroline and nitrogen analysis combination. Results of this study are proof of principle that the redox active iron-bearing mineral phases within soils are capable of removing nitrate from soils.

## TABLE OF CONTENTS

# CHAPTER ONE

# INTRODUCTION

## 1.1 THE NITRATE PROBLEM

Nitrate is an important inorganic nitrogen species, key to the healthy growth of all vegetation either through direct uptake or indirectly through processes involving a range of bacteria within the soil and root systems. Logically, this makes nitrate a target of most fertilizer regimens, with tons applied annually to fields in most all agricultural regions, primarily as ammonia. Combined with irrigation, rain, natural water tables and nitrate's high solubility, it is not surprising that nitrate contamination of water sources in human populated areas is widespread.

A litany of negative human health effects are attributed to these high levels of nitrate within our waters, including an increased risk of a number of cancers, chronic diseases and birth defects (Camargo & Alonso, 2006). Nitrate also contributes extensively to the acidification, eutrophication of, and hypoxia in, bodies of water in nearly every coastal region with significant human population by promoting algae growth. Hypoxia is especially of major concern in the Gulf of Mexico, particularly near the Mississippi River delta (Camargo & Alonso, 2006; Mississippi River/Gulf of Mexico Watershed Nutrient Task Force, 2007). Beyond the direct health and environmental stresses caused by nitrate, economic side effects can be felt in the strains on health care these issues pose and the loss of income in areas reliant on clean waters for fishing and tourism.

Nitrate pollution is, in large part, a side effect of the over application of nitrogen fertilizers. Until such time as the entrenched economic factors that still promote excess nitrogen application are addressed, methods of alleviating—or altogether eliminating—nitrate

contamination due to human activity by other means are naturally of interest for the above stated reasons.

Additionally, clean up and immobilization efforts at sites dealing with contamination by oxidation-reduction (redox) active heavy metals—cobalt, technetium, uranium—are hampered by the high levels of nitrate that are also present. Nitrate, sitting higher in the reduction series, must be dealt with first before any method of sequestration relying on redox reactions within the organic, inorganic, or both portions of the soil is attempted. To this end, understanding the interactions between nitrate with the redox active, iron containing portions of soils is necessary.

## 1.2 LITERATURE REVIEW

Much of the work focusing on nitrate and the nitrogen cycle within soils has focused primarily on bacterial processes. Beyond the microbial processes of denitrification and dissimilatory reduction of nitrate to ammonium, other means of reducing nitrate have been documented in nature that do not rely directly on bacteria. A sharp, dramatic drop in nitrate levels between the oxic and anoxic zones of Danish soil profiles has been observed, even though microbial denitrification is absent, thus demonstrating that an abiotic pathway for nitrate depletion exists in natural soils (Ernstsen, 1996; Ernstsen et al., 1998). This phenomenon is attributed to nitrate reduction by reduced Fe (ferrous iron) in the soil clay minerals, possibly Fe(II) produced by microbial reduction.

This seems reasonable as microbial reduction of iron in clay minerals is well known. Since the discovery that microorganisms are able to reduce structural Fe(III) in clay minerals (Stucki and Getty, 1986; Stucki et al., 1987; Komadel et al., 1987), many studies have confirmed this finding (Stucki and Kostka, 2006). Wu et al. (1988) showed that microorganisms in extracts

from Chinese rice-paddy soils actively reduce smectite structural Fe; and studies by Kostka et al. (1999a,b, 1996), Cervini-Silva et al. (2003), and Akob et al. (2008) reported that microorganisms from a variety of origins, including well-drained as well as flooded soils, can reduce structural Fe(III) in smectite and change its physical-chemical properties. Kim et al. (2003) demonstrated that microbial reduction causes clay layers to collapse, thereby showing a similar phenomenon to that observed in dithionite reduced smectites by Wu et al. (1989) and Shen and Stucki (1994).

As well, the involvement of clay minerals in these reactions would be no surprise because they are the most chemically active mineral fraction of soils and sediments, and their surfaces exert a dominant influence on chemical processes occurring there. The oxidation state of structural Fe in the clay has a profound impact on these physical and chemical properties (Stucki, 1988; Stucki et al., 2002, 2006). Among the properties affected are cation exchange capacity (Stucki et al., 1984a), cation fixation capacity (Chen et al., 1987; Khaled and Stucki, 1991; Shen and Stucki, 1994), surface area (Lear and Stucki, 1989; Kostka et al., 1999a), layer stacking order (Stucki and Tessier, 1991; Kim et al., 2003, 2004), surface pH (Cervini-Silva et al., 2000), site occupancy of Fe in the clay crystal (Manceau et al., 2000), swelling in water (Stucki et al., 1984c; Gates et al., 1993, 1998), and degradation of chlorinated aliphatic and nitroaromatic compounds (Cervini-Silva et al., 2001, 2002, 2003; Hoffstetter et al., 2003, 2006, 2008; Yan & Bailey, 2001). Any number of these properties could influence the reactivity of clay minerals towards the reduction of nitrate.

Methods of bacterial stimulation have been discovered and could be applied to effect reduction of iron within the soil. This in situ reduction by biostimulation of indigenous Fe-reducing bacteria in the soil can be achieved with addition of a carbon source and electron donor, such as ethanol or glucose, as reported by Stucki et al. (2007) and Akob et al. (2008). It has been

suggested that a class of iron species known as green rusts may be responsible for the nitrate reduction potential within soil environments. Green rust (layered Fe(II)Fe(III) hydroxide, GR) has been identified as an excellent reductant for nitrate. Although it is believed to exist in soils, it has not yet been well characterized even within the laboratory due to it being extremely redox reactive—even verifying its presence within a soil sample would require extreme care in obtaining the sample (Hansen et al., 1994, 1996, 1998, 2001).

In addition to the use of highly reactive synthetically prepared green rust compounds, several laboratory methods have been used to reduce and study nitrate and its reactions with reduced iron species. Concentrations of nitrate and its reduction products, nitrite and ammonium, may be monitored and calibrated through spectrophotometric instruments and other methods (Norman & Stucki, 1981; Mulvaney, 1996). By harnessing the reductive potential of the sulfoxylate radical formed in solution by the dithionite anion, a route for laboratory reduction of iron clay minerals in an oxygen free atmosphere was developed, as described by Stucki et al. (1984b). Experiments using ditionite as a reductant for clay minerals have shown that near complete reduction of ferric iron sites throughout the clay is possible if given enough time, heat and a headspace sweep of the reaction vessel (Komadel et al., 1990).

Clay minerals can also be reduced by using iron reducing bacteria (Kostka et al., 1996). Such samples could be used in experiments aimed at understanding conditions under which nitrate can be reduced by iron-containing clay minerals. This bacterial reduction does not approach levels possible through chemical reduction however, as it most likely occurs only at the edge sites, whereas dithionite reduces the entire structure from the basal surfaces (Figures 1-4; Ribeiro et al., 2009). The ubiquity of iron-reducing bacteria in a large range of soil types from many parts of the world points to them as a source of growing interest in such work.

Nitrate has also been shown to be directly reduced by atomic iron (Miehr et al., 2004; Alowitz & Scherer, 2002; Sianta et al., 1996; Till et al., 1998; Huang et al., 1998; Devlin et al., 2000; Westerhoff, 2003; Sohn et al., 2006). Nitrate has also been shown to be catalytically reduced by iron(II) in the presence of copper(II) that is bound to the surface of iron oxides. As well as copper(II), cadmium(II), silver(I) and nickel(II) were also shown to have catalytic properties in nitrate reduction in conjunction with iron(II), pointing to a conclusion of naturally occurring abiotic nitrate reduction as a very real phenomenon (Ottley et al., 1997).

Nitro groups in nitroaromatic compounds act as an analog for nitrate. Evidence of abiotic soil reduction of nitrate stems from experiments by Hofstetter et al. (2006) showing that goethite spiked with Fe(II) is capable of nitroaromatic reduction. Reduction of nitroaromatic compounds has been observed by another class of compounds of interest. The reduced quinones jugalone and lawsone have been shown to possess a pH-dependent capacity for reducing mono-substituted nitrobenzene and nitrotoluene compounds (Schwarzenbach et al., 1990). Once again, the ability to reduce nitroaromatic compounds points toward a possible method of reducing nitrate.

More recent studies have shown that an important anaerobic pathway of some bacteria is the reduction of other quinones, in particular anthraquinone-2,6,-disulfonate (AQDS) (Cervantes et al., 2008). The reduction products of AQDS, anthrahydroquinone-2,6,-disulfonate and anthradihydroquinone-2,6,-disulfonate (abbreviated AHDS, AHQDS and/or $AH_2QDS$ depending on author), have been shown to be active reductants, just as jugalone and lawsone. AHDS, both alone and in the presence of bacterial cells, reduces the explosive hexahydro-1,3,5-trinitro-1,3,5-triazine to various nitroso products. Once again, this quinone-mediated reduction was shown to be pH dependent (Kwon & Finneran, 2008). Several quinones, including AQDS, are active participants in bacterial denitrification as well (Aranda-Tamaura et al., 2007). Borch et al. (2008)

found that the reductive ability of AQDS comes from its role as an electron shuttle. In this capacity, AQDS is reduced to AHDS by ferrihydrite that has previously been reduced by bacteria. AHDS is then oxidized back to AQDS by nitroaromatic compounds.

To date, no articles in the literature have dealt directly with the interactions of nitrate and reduced clay minerals. The following study seeks to determine the efficacy of redox-active, iron-rich clays—as an analog for minerals in systems found in nature—to reduce nitrate. This is but the first step towards understanding the complex interactions that clay minerals have with this ubiquitous, naturally occurring and human amplified nitrogen species.

## 1.3 HYPOTHESIS & OBJECTIVES

The work hereafter described is based upon the hypothesis that reduction of structural Fe in soil clay minerals, whether by bacterial or chemical reducing agents, creates a reduction potential at the mineral surface that is conducive to nitrate reduction and that the rate of reduction is sufficient to remove nitrate from the targeted systems. Considering both the thermodynamics and kinetics of these redox processes is essential for such natural systems.

As well, this work examines the abiotic electron shuttle capacity of AQDS in nitrate reduction. Iron clays reduced by dithionite or by bacteria may reduce AQDS, which may in turn reduce nitrate. It seems logical to hypothesize that reduced iron produced through abiotic processes should be capable of making use of the electron shuttling properties of AQDS to reduce nitrate just as bacterially reduced iron species use electron shuttling or that bacterially reduced iron may do the same when no longer in the presence of a bacterial mediator.

Furthermore, as metallic Fe is well known as a reductant for nitrate and more recent studies also show that it is capable of reducing structural Fe in clay minerals, this study seeks to

investigate whether the addition of Fe(0) to a clay mineral suspension will produce a reduced-Fe mineral phase that is highly reactive toward the reduction of nitrate. This scenario may create a system in which both reducing capacity and catalytic activity are enhanced and, thus, could represent the optimum conditions.

# CHAPTER 2

# METHODS

## 2.1 SAMPLE PREPARATION & REDUCTION

All experiments were performed using the Source Clays Repository recognized ferruginous smectite, SWa-1—hereto forward referred to as "SWa-1" and "clay" within the methods section for ease of reading. All water used was first purified by a Barnstead Fisher NanoPure System Model D4741, fed by a DI water source.

Each experiment described was performed in triplicate, up to section 2.6, with each reaction in a separate 50 mL polycarbonate centrifuge tube. The centrifuge tubes' two piece sealing tops and screw caps were modified by addition of a small hole drilled through the center of each. Rubber septa were inserted between the two cap pieces, allowing for needles to be inserted while maintaining an airtight seal around a tube's contents.

Each sample tube received a fresh preparation of citrate-bicarbonate buffer from stock solutions for each trial. The buffer components were 5 mL 0.18 M sodium citrate (Fisher Scientific, Waltham, MA) in water, 10 mL 0.36 M sodium bicarbonate (Fisher Scientific, Waltham, MA) in water, and an additional 15 mL of water. Final buffer concentrations were 0.03 M sodium citrate and 0.12 M sodium bicarbonate in a 30 mL total volume. Into each tube was then weighed a 50 mg sample of SWa-1. Tubes were capped and mechanically vortexed for 20 minutes, suspending their contents.

Tube contents were chemically reduced using sodium dithionite (Mallinckrodt Baker, Lopatcong Township, NJ). A 200 mg portion of sodium dithionite was weighed and added to the C-B clay suspension in each reaction tube, after which the tube was immediately septum sealed and placed in a 70 °C water bath. Two needles were inserted through the septum modified cap.

One needle brought nitrogen gas, passed through an oxygen trap, into the tube; the second needle vented excess gas, purging gaseous reaction products (e.g. $H_2S$) from the system. Because the mass of reductant added to each reaction was constant, the extent of reduction was controlled by reaction time within the water bath. Reactions were quenched by submersion of the tubes in liquid nitrogen. Experimental runs were defined by these reduction times as follows: 10 minutes, 30 minutes, 1 hour, 4 hours and an unaltered control group that was not reduced. After quenching, tubes were centrifuged at 19000 rpm (18000 g) for 20 minutes in a Sorvall RC 50 Plus.

## 2.2 WASHING

Samples were washed in a custom designed apparatus (Figure 5), which allows for the oxygen-free transfer of liquids to and from redox sensitive systems. At its core are two large flasks, one filled with a 5 mM sodium chloride (Fisher Scientific, Waltham, MA) solution in water and the second with pure water (18 MOhm-cm). Each flask sits on a stirring hot plate and is equipped with a magnetic stir bar, wide central neck, and four smaller, threaded necks equipped with ACE Threads for rigid tube access.

Each of the four threaded necks on the flasks serves a different purpose. One allows access to the flask solution by a gas dispersion tube through which $O_2$-free $N_2$ is passed to purge the solution. Another is for an open-ended tube submerged well into the liquid, through which the solution is extracted via a 3-way valve, described later. The third threaded neck is connected to a vacuum source, and the fourth is equipped with a pressure relief valve (10 psi). A condenser coil is attached to the central neck of each flask, which is used for rapid cooling of the solution after boiling. Above the whole flask at the central neck is a water jacketed condenser column.

The top of the condenser column is attached to the bottom of a 3-way stop cock which is continuously swept with nitrogen while maintaining the flask contents at atmospheric pressure.

This design allows the flask contents to be purged of oxygen by bubbling nitrogen through the gas dispersion tube while boiling the solution. Opening the stop cock at the top of the condenser column so that all three branches are interconnected allows the purge gas to escape while sweeping the outlet with nitrogen, thus preventing any back draft of oxygen from the atmosphere. Water is condensed out of the purge gas as it rises through the condenser column. The deoxygenation process is more effective if the solution is boiled and stirred because the solubility of oxygen in water decreases with increasing temperature. When heating, the condenser column must be operating properly to prevent water from escaping and collecting in the vent line. If solutions have been deoxygenated recently, 30 minutes of heating is sufficient for re-deoxygenation. If, however, solutions have been replaced, at least an hour of heat and nitrogen bubbling is necessary. After heating is finished, the condenser coil in the solution is turned on to cool the flask contents; nitrogen bubbling through the flasks and head space sweeping should not be terminated for approximately 15 minutes after heating is stopped to prevent an overpressure of water vapor. When nitrogen is no longer needed, the lines are closed and the 3-way stop cock rotated to bypass the flask and condenser column.

Once the solution is properly deoxygenated and samples have been centrifuged, they can be washed without exposure to the atmosphere by inserting the two syringe needles from the apparatus through the septum cap. One needle is used for decanting the supernatant solution, which feeds through a Tygon tube into a large neck filter flask under vacuum. When inserted through the septum cap of the centrifuge tube, this needle pulls gases and liquids from the tube, allowing the supernatant liquid to be collected in the filter flask either to be analyzed or

discarded later, leaving the solids behind. The second needle is attached to a 4-way valve. In position 1 the needle is closed. In position 2 it feeds nitrogen from the previously described cylinder through the needle. Position 2 is used when removing the tube contents with the vacuum needle, replacing the liquid volume with nitrogen to prevent negative pressures inside the tube relative to the ambient atmosphere so that air from the atmosphere is not pulled into the tube, contaminating the sample. In position 3 the needle becomes another vacuum needle. In position 4 the needle is connected to a multi-port valve which allows connection to the solution-extraction tube inserted into and of four different flasks containing deoxygenated solutions. Using the flask selector valve, a line can be opened to either flask through the unobstructed glass tube in one of the threaded flask necks which is controlled by the earlier mentioned 3-way valve. In position 1 on this 3-way valve, the line is closed. In position 2 the line is open and the flask solution is pulled through the line due to the vacuum being applied by the vacuum needle. If the pressure differential between the flask and the centrifuge tube is too little, the 3$^{rd}$ position on this last switch pushes nitrogen through the unobstructed tube, clearing it and creating a positive pressure of nitrogen inside the flask.

The washing of the reduced clay samples after centrifugation removes any remaining sodium dithionite and any associated byproducts. The citrate-bicarbonate buffer is replaced with 5 mM sodium chloride from the first flask, after which the tube is vortexed and shaken until its contents are suspended in the new solution. After suspension, samples are again centrifuged at 19000 rpm for 20 minutes, the supernatant removed and a second portion of 5 mM sodium chloride is added. The third wash also uses the sodium chloride solution. The fourth wash uses the second flask's pure water (18 MOhm-cm). After centrifugation, the supernatant is removed

but not replaced, leaving a small amount of reduced clay in an atmosphere of nitrogen within the tube.

## 2.3 IRON ANALYSIS

The washed clay with little remaining supernatant removed was next analyzed for ferrous and total iron content using a 1,10-phenanthroline and UV light method, modified slightly from Komadel & Stucki (1988). Analysis runs averaged between three and six washed clay samples, representing one or two different reduction time trials, as well as four standards to verify the accuracy of the analysis.

Each standard was prepared in a polycarbonate centrifuge tube identical to the reduction reaction tubes. Tubes were labeled according to their approximate iron concentrations after final dilution as 0 ppm, 1 ppm, 3 ppm and 5 ppm. The mass of each empty tube was recorded and into each approximately 7 mg of ferrous ammonium sulfate (Allied Chemical and Dye, New York, NY) was weighed per integer of final desired concentration in ppm. The weight of the tube and the standard were recorded so exact concentration could be determined during data work up. After standard weighing, all white lights in the room where the analysis was being performed were turned off in favor of red lights. This prevented ferric iron in samples, which also forms a complex with 1,10-phenanthroline, from being photo-chemically reduced before ferrous iron concentrations had been determined.

Digestion and complexing reagents were added in fast succession to each standard and sample to minimize reoxidation of the reduced clay samples in the presence of air; reduced clay samples were only uncapped just before addition of digestion reagents. A 12.0 mL aliquot of 3.6 N sulfuric acid produced from concentrated sulfuric acid (Mallinckrodt Baker, Lopatcong

Township, NJ), a 2.0 mL aliquot of 10% by weight 1,10-phenanthroline (Sigma-Aldrich, St. Louis, MO) in 95% ethanol, and 1.0 mL of 49% hydrofluoric acid in water (Acros Organics, Geel, Belgium) were added to all standards and samples. The centrifuge tubes were placed in a boiling water bath for 30 minutes to digest their contents, followed afterwards by a 15 minute cooling period. Once cooled, 10.0 mL of 5% by weight boric acid (Acros Organics, Geel, Belgium) in water was added to each centrifuge tube.

Centrifuge tube contents were quantitatively transferred to 100 mL polypropylene tubes, which had previously been weighed while empty. Each of these "iron analysis tubes" was filled to within an inch of its top with water and its final mass recorded. A piece of parafilm was placed securely across the top of each tube to prevent spilling and the tube was then inverted several times to induce mixing. After mixing, a Brinkmann Dosimat dilutor drew a 2.0 mL aliquot of the tube's contents and expelled them into a 50-mL Erlenmeyer flask along with 20.0 mL of 1% by weight sodium citrate solution in water. Two such flasks were produced from each iron analysis tube for duplicate absorbance measurement.

Final solutions were analyzed on a Varian Cary 5 UV-Vis spectrophotometer equipped with a Routine Sampling Accessory (RSA) Internal Sipper using the Concentration software application provided by Varian. The spectrometer was allowed to warm up for a minimum of 30 minutes prior to zeroing and sample analysis. The absorbance at 510 nm of the ferrous iron and 1,10-phenanthroline complex was measured, with two replicate measurements taken from each flask. During ferrous iron analysis the room was illuminated with only subdued red light, and the sipper line was rinsed twice with water between samples to prevent cross contamination. After absorbance values were collected for ferrous iron, all flasks were placed in an enclosure with two

high intensity mercury vapor lamps for 2 hours to reduce the ferric iron complex. The total iron absorbance values were then measured at 510 nm.

## 2.4 NITRATE ADDITION

A second group of reduced, washed clay samples from each reduction-time set were identically prepared to be reacted with nitrate. An 88 μM solution of sodium nitrate (EM Science, Gibbstown, NJ) was prepared in water. For each sample a 20.0 mL aliquot of nitrate was prepared in a capped centrifuge tube. Each was deoxygenated by flowing nitrogen into the solution for a minimum of 30 minutes through a needle which penetrated the septum cap, venting excess gas through a second needle. Nitrogen flow was continued while the aliquot was drawn from the centrifuge tube by a gas tight syringe and injected into a tube containing the washed, reduced clay, also equipped with nitrogen and vent needles.

After injection, the clay was suspended in the nitrate solution by mechanical vortex and then tubes were placed on a shaker plate for 18 hours. Samples were then centrifuged and affixed with a nitrogen needle and vent needle in the headspace, so as not to disturb the supernatant liquid or the collected solid at the bottom. The supernatant was carefully removed by gas tight syringe, and placed in new tubes which were frozen for shipping to be analyzed for $NO_x^-$, nitrite and ammonium as described below. The remaining clay was analyzed by the 1,10-phenanthroline method for iron content to compare with samples not reacted with nitrate.

## 2.5 NITROGEN SPECIATION ANALYSIS

Nitrite and nitrate were analyzed together using a modification of the method described by Braman & Hendrix (1989) to determine $NO_x^-$ concentrations using a Thermo Model 42i

Chemiluminescence Analyzer. The sample holder on the instrument was filled with 100 mL of acidified (1-2 M HCl) 0.10 M vanadium (III) solution, bubbled with helium. Instrument response was calibrated by 100 μL injections of $NO_x^-$ standards ranging in concentration from 1 to 50 μM. Evolved NO was carried by helium flow to the analyzer and the peak area recorded. Sample injection volume was varied between 50 and 200 μL.

Nitrite alone was measured using a modified Garside (1982) method. The method was modified such that it was identical to the combined nitrite and nitrate method described above with the exception of the reagent solution in the sample holder. The nitrite only mixture is a 1:3:6 ratio of 3% w/v sodium iodide in water, glacial acetic acid, and pure water. Calibration and sample analysis were carried out as above.

Ammonium concentrations were determined by a colorimetric modified Berthelot method as described by Bower & Holm-Hansen (1980). A 1.0 mL portion of each sample or standard solution is mixed with 0.12 mL of a salicylate catalyst solution composed of 440 grams of sodium salicylate and 0.28 grams of sodium nitroprusside per liter of water. To this was added 0.2 mL of an alkaline-hypochlorite solution, a 1:10 mixture of commercial bleach and a solution containing 18.5 grams of sodium hydroxide and 100 grams of sodium citrate per liter of water. Samples were placed in a dark area for 1 hour and then their absorbance measured at 640 nm on a Shimadzu UV mini 1240. Standards ranged from 1 to approximately 53 μM concentration.

## 2.6 FLOW REACTOR EXPERIMENTS

### 2.6.1 UV-Vis Nitrate Quantification Method Development

To measure changes in nitrate concentration in house, it was attempted to create a UV-Vis method of quantifying nitrate and nitrite levels. Early on, it was recognized that two distinct

absorbance peaks for nitrate exist: a broad band centered at 300 nm that appears at concentrations of approximately 0.50 mM and upwards, and a narrow band centered at approximately 210 nm (Figure 6). The 210 band was chosen for use, both because the 300 nm band becomes washed out when coupled with a clay suspension which absorbs highly in this region, and because the nitrate concentrations being used in experiments were small enough that the absorbance band at 200 nm was not too high and the 300 nm band was nonexistent.

The next logical step in creating this method was to obtain the spectra of likely reduction products of nitrate—nitrite and ammonium—in the region of the main nitrate peak. Ammonium lacks any absorption in the relevant UV spectral region, while nitrite (Figure 7) has a similar absorption peak but at a slightly longer wavelength, approximately 210 nm. The peaks are differentiable as can be seen in the side by side comparison (Figure 8). Peak separation software may be used to render the peaks apart from each other in a solution in which both are present in low concentrations.

A pump flow reactor was set up so that the spectrum of a reaction could be monitored over time without error introduced from sample loss or air introduction during sample extraction and transfer. The reactor consisted of a 50 mL centrifuge tube modified with a port added to the bottom and another to the top, just below the cap threading. The bottom port was connected by tygon tubing to a variable speed peristaltic pump. The pump fed a 1 cm path length cuvette equipped with inlet and outlet ports; the outlet of the cuvette ran back to the upper port on the centrifuge tube. The same modified caps allowing for nitrogen gas addition and purge described earlier were used. This allowed for the system to be flushed of air with nitrogen prior to the addition of any oxygen-sensitive reagents or samples.

### 2.6.2 Bacteria Reduced Clay & AQDS

A suspension of SWa-1 reduced by *Geobacter daltonii* strain FRC-32, obtained from the lab of Professor Joel E. Kostka, was used to test the reactivity of a naturally reduced clay toward nitrate. The bacteria-clay suspension was kept in an inert atmosphere within a glove box to prevent oxidation. Drying a 5 mL sample in an oven for several hours revealed it to contain 20.58 mg of clay per mL.

A 25.0 mL aliquot of approximately 0.025 mM nitrate solution was added to the pump reactor and deoxygenated under nitrogen atmosphere as described above. An 8 mL sample of the bacteria-reduced clay was added via a gas tight syringe. The flow direction on the peristaltic pump was set in reverse, bubbling nitrogen through the tube contents and mixing them. The flow direction was then set to forward and the absorbance value of the solution was collected every 30 minutes for 12 hours from 190 to 400 nm.

This experiment was also performed for bacteria reduced clay in the presence of AQDS. A 25 mL portion of 0.025 mM nitrate solution was pH buffered as described by Kwon & Finneran (2008) by addition of 62.5 mg of sodium hydrogen carbonate (Fisher Scientific, Waltham, MA) before sparging with nitrogen to remove oxygen before addition of approximately 5 mg of AQDS, acquired from the lab of Professor Kevin Finneran. The buffered nitrate and AQDS solution were placed in the flow reactor, the contents of which were then further sparged to remove oxygen from the air space within. A 4 mL portion of bacteria-clay suspension was added, the contents of the tube mixed, and the spectrum observed for 12 hours. Similar experiments were performed for comparison using 50 mg of clay in citrate-bicarbonate buffer reduced by 100 mg of dithionite at 70 °C for 2 hours with AQDS.

A separate set of experiments was performed to independently verify these results. Experiments represent dithionite-reduced clay alone, dithionite-reduced clay with AQDS, bacteria-reduced clay alone, and bacteria-reduced clay with AQDS. Bacteria samples were 5 mL in volume, centrifuged at 16000 (12900 g) rpm for 30 minutes, and the supernatant liquid discarded. Aliquots 20.0 mL in volume of deoxygenated 0.025 mM nitrate were introduced into all samples before overnight agitation (12-14 hours). Tubes were centrifuged and the supernatant liquid transferred by gas tight syringe to new centrifuge tubes which were frozen and shipped for nitrogen analysis as described above. The remaining solids were analyzed for ferrous and total iron, as were samples of the dried bacteria-clay suspension and dithionite-reduced clay representing the reduction state used in these experiments.

### 2.6.3 Zero-Valent Iron

In order to create an environment in which both reduced clay and other iron oxide species would be present, zero valent iron was used as a reductant. Two samples were prepared in 50 mL septum-capped centrifuge tubes each containing 50 mg of SWa-1 and 10 mg of Fe(0) in 30 mL of water. One sample, hereafter referred to as “deoxygenated,” was purged with nitrogen and wrapped in parafilm to prevent reintroduction of oxygen. The second sample, “oxygenated,” had a needle pierced through its septum cap to allow exchange of its contents with the atmosphere. Both samples were reacted for 20 days.

After reaction, the oxygenated sample was transferred to the pump reactor along with 25 mL of 0.025 mM nitrate solution. The contents were circulated under nitrogen atmosphere for 12 hours, with the spectrum recorded every 30 minutes. The deoxygenated sample was then transferred via a gas tight syringe to the pump reactor and 25 mL of 0.025 mM nitrate solution

that had been previously sparged with nitrogen was added. The contents were circulated for 12 hours and the spectrum recorded every 20 minutes.

# CHAPTER 3

# RESULTS & DISCUSSION

## 3.1 Iron Analysis

Following each iron analysis trial, absorption values for the standards were plotted against their known iron concentrations to create calibration curves. Curves were used to verify both that the method returned a linear response within the concentration range and that the specific trial set was responding properly. Calibration curves constructed for both iron(II) and total iron for a single trial run (Figures 9 and 10), were uniformly linear with correlation coefficients within the same range as those in the figures, excepting one trial with an outlying standard.

Accuracy and precision were also correlated across the entire experimental range using the Beer-Lambert Law, $A = \varepsilon \bullet c \bullet l$, where $A$ is the absorption value, $\varepsilon$ is the absorptivity coefficient in $M^{-1}cm^{-1}$, $c$ is the molar concentration and $l$ is the path length of the cell used. Using the known concentrations of the standards analyzed in each trial in conjunction with the absorption values obtained and the 1 cm path length of the cuvette used in the UV-Vis spectrometer in all experiments, the absorptivity of all standards was calculated (Table 1). The absorptivity values were averaged, excluding a single outlier, resulting in absorptivity coefficients of 931 $M^{-1}cm^{-1}$ ± 5% for Fe(II) and 1044 $M^{-1}cm^{-1}$ ± 4% for total Fe. The slightly higher value of the total Fe absorptivity coefficient versus that of Fe(II) is in agreement with the findings of Komadel & Stucki (1988).

Using the absorptivity coefficients derived from the standards, the Beer-Lambert law was again used to calculate the concentrations of ferrous and total iron present in the sample solutions. The concentrations are normalized by dividing by the mass of clay used in each trial,

and then these values are averaged across each time set and a ratio between ferrous and total iron is derived (Table 2).

The "unaltered" samples—those that had not been reacted with dithionite—show only a trace amount of ferrous iron which is negligible compared to the total iron content. The amount of ferrous iron present in the unaltered samples is the same both before and after reaction with a dilute nitrate solution. The remaining sample sets in the before nitrate reaction group have consistent total iron concentrations from 1.63-1.98 mmol Fe/g clay. The total iron values after reaction with nitrate are likewise consistent within themselves, but showing a slight decrease spanning 1.43-1.56 mmol Fe/g clay.

After only 10 minutes of reduction in the presence of dithionite, the ferrous iron content increases dramatically accounting for roughly a quarter of the total iron in the structure. Following reaction with nitrate, the ferrous content of the 10-minute trials does not drop significantly. Interestingly, the extent of reduction in the 30-minute samples and the 1-hour samples is similar, with both falling in the 50-60% range. The values after introduction to nitrate are likewise similar to each other, but a large amount of reoxidation is evident in both cases. After 4 hours of reduction, nearly all ferric iron in the clay structure is converted to ferrous iron. When coupled with the values shown for 10, 30, and 60 minutes, it appears that a large amount of reduction occurs in approximately the first 30 minutes of reaction and the rate of the reaction significantly decreases after this point.

The 4-hour samples exhibit the most reoxidation in the presence of nitrate, decreasing from 89% ferrous iron to 52%. It should be noted that the 4-hour samples are not reoxidized to the same extent as the 30-minute and 1-hour samples, which in turn are not as reoxidized as the 10-minute samples. This suggests that the structural ferrous iron is not all available to be reacted

with nitrate. This may in large part be due to the random reduction of iron sites at the basal surface. The nitrate anion is unlikely to react at the basal surfaces due to coulombic repulsion, and therefore is left only with the ferrous iron at the comparatively smaller surface area available at the edge sites due to the random reduction of the clay structure achieved by use of dithionite. If so, some form of electron transfer to the edge sites is necessary for the complete reoxidation of the clay structure.

Iron analysis results for the bacteria and AQDS experiments (Table 3) were calculated on a mmol of iron per gram of clay basis as well. While the initial ratio of ferrous to total iron within the bacteria-reduced clay is low, it is important to note that the vast majority of these ferrous sites are located at, or in very close proximity to, the clay edge due to the mechanism of bacterial reduction. These sites are potentially more available than the larger number of ferrous sites produced by the chemical reduction conditions used within these experiments. With this in mind, it is unsurprising to see the near complete reoxidation of the clay structure. Bacteria without the addition of the electron shuttle AQDS were perhaps slightly less effective than when paired with AQDS, but the differences in ferrous iron content are negligible. So too are the differences between the dithionite treatment with and without AQDS. Iron analysis data alone of the clay before and after reaction does not yield enough information to make a pronouncement on whether or not AQDS has an impact upon clay reactivity toward nitrate, but it does suggest that AQDS retards the reaction when coupled with chemically reduced clay. Iron analysis of the bacteria-reduced appears to support the initial hypothesis that AQDS promotes the reaction, however the difference in ferrous iron content between the bacteria-reduced trial with AQDS and the trial without AQDS is negligible. Iron analysis alone cannot confirm the hypothesis in this case.

## 3.2 NITROGEN SPECIATION

The nitrogen speciation tests for the variably reduced clay samples (Table 4) show that the general trend is for $NO_x^-$ values to decrease from their original 88 μM concentration as the extent of reduction in the clay increases. An unexpected slight decrease in $NO_x^-$ concentration within the Unaltered samples, comparable to that in the 10 minute samples, suggests that there is a slight error in the method of approximately ± 1.5 μM. No nitrite appears in the solutions of the Unaltered samples, confirming that no nitrate was likely lost from the unaltered samples. Nitrite concentrations among all reduced samples are extremely low and comparable with one another. Nitrite, therefore, is not a major reduction product in these reactions: far more $NO_x^-$ is lost relative to how much of the remaining $NO_x^-$ is nitrite. Furthermore, nitrite concentrations do not increase with increase in extent of reduction or with total nitrate reduced (Table 5). Nitrate remaining is calculated as nitrite values subtracted from $NO_x^-$ and total nitrate reduced is the calculated nitrate concentration subtracted from the initial concentration in the nitrate solution used of 88 μM multiplied by the volume of the aliquot introduced to the sample, 20 mL.

Although the data presented make it clear that nitrite is not a significant reduction product, or at the very least that large concentrations of nitrite do not build up due to further reduction, the data from the variable reduction time experiments do not present any clear information about ammonium. A slight green tint present in the sample solutions which may have been due to clay dissolution prevented the colorimetric ammonium determination method from being performed accurately. It was attempted to dilute the solutions to overcome the color contamination, but the concentrations of ammonium present were too small to be effectively detected.

Nitrogen speciation results from the bacteria and AQDS experiments (Table 6) shed some light on the levels of ammonium produced in dithionite-reduced samples. Detected ammonium levels within the dithionite and dithionite with AQDS samples are much higher than the nitrite levels, which in turn are uniformly low across both trials just as in the variable reduction time experiments. It also bears noting that if the combined $NO_x^-$ and ammonium numbers here represent all nitrogen species (ie: no reduction to dinitrogen or other gaseous nitrogen species) then the initial concentration of the nitrate used was 0.030 mM not 0.025. This conclusion cannot be supported without knowledge of the possible gas phase nitrogen products that may have formed in the reaction, so an initial concentration of 0.025 mM nitrate is maintained.

Nitrogen analysis shows that the presence of AQDS in the reaction medium does not promote a reaction between nitrate and the chemically reduced clay, as did the iron analysis. Quite the opposite, the data collected point toward the conclusion that AQDS in fact retards the reaction. Ammonium and nitrite levels in the trials using dithionite but not AQDS are higher than in those with AQDS while remaining nitrate levels are lower. This, coupled with the iron analysis results indicating a greater ratio of ferrous iron remaining in the reaction involving dithionite and AQDS, show that AQDS does not have the hypothesized electron transport synergy with the chemically reduced clay.

The bacteria and bacteria with AQDS results are more difficult to analyze. In retrospect, it is obvious that the nitrogen compounds within the bacteria themselves lend extensively to the levels detected by analysis methods. While this makes the data unusable quantitatively, if it is assumed that because the same amount of the bacteria-clay suspension was used in both the experiments with and without AQDS, then the bacteria present are essentially the same and will

provide roughly the same background nitrogen levels Making these assumptions, a qualitative comparison is possible. Approaching the data in this way, it can be concluded that AQDS, when paired with the bacteria reduced clay, does indeed promote the reduction of nitrate. The nitrate concentration of the trial using AQDS is lower than that without, while the nitrite and ammonium concentrations are greater. Unfortunately, without a means of differentiating bacteria-associated nitrogen from the nitrogen introduced for reaction, it is impossible to reach any conclusions with the nitrogen speciation method pertaining to the differences in reactivity between chemical and bacteria reduced clay besides those concerning the effect of AQDS.

Looking at the nitrogen speciation and iron analysis together as a whole it is clear that, as hypothesized, chemically reduced clay is very much capable of nitrate reduction. By plotting the amount of ferrous iron initially available against the amount of nitrate reduced (Figure 11), a clear trend between the extent of reduction within the clay structure and the amount of nitrate that is reduced is visible. The points are not perfectly colinear, but as noted before the state of reduction within the structure is such that not all ferrous iron is available for reaction at the edge sites. Combining these points with the amount of nitrate removed from the original solution in the dithionite trial of the bacteria and AQDS experiments (Figure 12) shows that the trend remains. This result is quite significant, given that this experiment was carried out independently of the variable reduction time trials, that the reduction state obtained was unique due to a different amount of dithionite being used for a wholly different amount of time, and that the initial nitrate concentration was different. This leads to the conclusion that the amount of nitrate that can be reduced over a short period of time depends only upon the reduction potential within the clay and not upon the concentration of nitrate present.

## 3.3 FLOW REACTOR EXPERIMENTS

Measuring the absorbance spectrum of samples in the flow reactor yielded spectra with two distinct peaks (Figure 13). This initial spectrum for dithionite reduced clay and AQDS within the nitrate solution shows that the hypothesized method of determining nitrate and nitrite concentrations may be confounded. The nitrate and nitrite peaks, at the concentrations present, are at no point in the 12 hour reaction period separable (Figure 14). This is compounded by the appearance of a third peak: the ferric-oxygen charge transfer band at 255 nm (Figure 15). Due to the overlap of the two bands, little can be inferred from these raw spectra alone. It can be seen that no nitrite shoulder appears on the nitrate band, so nitrate removal can be measured solely on the basis of the decrease in the nitrate peak. Separating the peaks and plotting the individual peak heights against time shows that the nitrate peak (Figure 16) does decrease rather rapidly over the first hour, and then progresses more slowly before returning to the level it achieved after one hour. The reasons for the nitrate levels returning are unclear. The ferric-oxygen charge transfer peak plotted over time (Figure 17) does not show the logically expected steady increase as oxidation, and therefore ferric iron concentration, increases.

The nitrate peak for the bacteria only flow reactor experiment (Figure 18) decreases exactly as expected. However, the paired ferric-oxygen charge transfer band (Figure 19) is once again highly scattered. The discernible trend within the scatter is for a decrease in the charge transfer band, conflicting with both the decrease in apparent nitrate concentration and the expected trend. Results from the bacteria with AQDS trial are very similar to the dithionite with AQDS trial. The nitrate peak (Figure 20) decreases very rapidly over the first hour and then fluctuates, predominantly hovering around the low point obtained after the first hour. The ferric-oxygen charge transfer band (Figure 21) is highly scattered, with no apparent increase or

decrease observed over the complete span of the reaction. The deoxygenated mixture of zero-valent iron and clay (Figures 22 and 23) shows a high amount of scattering for nitrate with no appreciable change over time, while the ferric iron content jumps dramatically in the first hour and then slowly rises for the remainder of the reaction. The oxygenated mixture of zero-valent iron and clay (Figures 24 and 25) shows a confounding steady increase in both nitrate and ferric iron content.

Overall, there is a lack of any consistency in the results from the flow reactor experiments. The inability to regularly obtain data that followed trends throughout a trial, let alone data that matched well from trial to trial, is the reason that flow reactor experiments were abandoned in favor of the combined nitrogen and iron analyses. As a means to obtaining both quick and reliable nitrate kinetics data in a system that absorbs in a similar region as nitrate, the pump and UV-Vis spectrometer combination fails to achieve. It is possible the system could be improved upon. Trapped nitrogen bubbles within the tubing may account for some of the fluctuation in readings. Although the minimum path length of tubing was used for the equipment available, it is possible that the reaction proceeded at different rates in the fairly spread out reaction mixture. Using equipment designed for the purpose of short and fast transfer of the reaction mixture to and from the cuvette could increase precision within any single trial. These suggestions do not account for methods of dealing with the confounding nature of the results obtained in some trials, especially those dealing with zero-valent iron.

While the author is hesitant to draw any conclusions from such mismatched data as the flow reactor experiments present, several of the trials exhibit trends that are verified by the nitrogen and iron analyses in the variable reduction time experiments that were conducted later. In the trials involving dithionite with AQDS as well as bacteria alone and with AQDS, nitrate

levels declined overall from start to finish. In two of these, the reaction appears to have proceeded quickly within the first hour or so and then to slow and possibly stop afterwards. This may be evidence of the postulated edge-site only reactivity of the reduced clay; any further reduction that occurred in these trials was slowed significantly by the need to transfer electrons from the inner structure to the clay edge. This may find further support from the extremely fast initial increase in ferric iron content in the deoxygenated zero-valent iron and clay mixture trial. This support is even more tentative than that from the dithionite and bacteria trials due to the lack of further experiments involving zero-valent iron with which to compare the peculiar data sets.

# CHAPTER 4

# CONCLUSION

Taken together as a whole, the experiments described previously provide evidence that microorganisms in soil may not be solely responsible for the reduction of nitrate. Initial experiments using the flow reactor, while providing very little in the way of quantifiable data, were able to provide an amount of support to this hypothesis. It may be possible in the future to elaborate on this method using equipment suited better to such an application, including a shorter path length in the tubing as suggested earlier or a spectrometer designed for better sensitivity in the near UV region.

Unquantifiable as it was, the data from the flow reactor experiments showed that a more rigorous approach must be taken. This led to the design of the combined iron analysis and nitrogen speciation experiments. Beginning with the same set of reaction conditions, minus the zero-valent iron trials, this quickly proved a much better source of quantitative data, the one exception being the bacteria reduced samples. Nitrogen speciation proved difficult for these samples as the bacteria themselves contain significant amounts of the nitrogen compounds samples that interfered with the analysis. Lacking a means of screening the bacteria background, continued trials involving bacteria reduced clay were abandoned. Given the time and cost involved with shipping samples for analysis, as done in the current study, obtaining the necessary equipment for further nitrogen speciation in house is needed.

The inability to effectively evaluate nitrate concentrations may just as well have been a boon. Dithionite-reduced clay was easily proven to reduce nitrate by this first use of the combination of iron analysis and nitrogen speciation. Removing the bacteria variable would allow experiments to quantify how the extent of reduction influences nitrate removal. The more

statistically rigorous variable reduction experiments were the result of this. These show a very strong correlation between the amount of ferrous iron available within the structure of a reduced clay mineral and its ability to reduce nitrate. When the five data points from this study are paired with the dithionite only trial from the initial run of the combined analysis the correlation holds and, in fact, seems even more linear. Once again, being able to run the nitrogen speciation in-house would greatly increase the efficiency in such analyses.

The combined analysis could also be adapted to a future study of the kinetics of these reactions, since the dynamic approach offered by the flow reactor does not work in this application. Duplicate samples would need to be prepared for each time step so as to allow both iron analysis and nitrogen speciation. The ability of iron analysis samples to survive over short periods of time and the fast nature of the nitrogen analysis would allow for time range of at least 10 hours in a study tracing the initial response of the system. As stated earlier, removing the bottleneck in freezing and transporting samples for nitrogen analysis is essential.

Having laid the groundwork for a more complete understanding of the interactions between reduced clays and nitrate, it seems plausible that continued work will soon allow for effective remediation efforts to be implemented. This could take the form of biostimulation of iron-reducing bacteria which are far more common in many soils than denitrifiers, enclosed redox-based effluent treatment modules (e.g. filters) for tile drainage systems, or others still. Iron bearing clay minerals most certainly have a large potential for rectifying contamination of water and soils by nitrate.

Whatever the form of future research or remediation efforts in this vein of research, it is now abundantly clear that iron-bearing mineral phases are an integral part of the redox pathways that govern the fate of nitrate. While it was known that bacteria action was not solely responsible

for nitrate removal from soils, little work had been done concerning this hypothesized method of reduction. Processes involving green rusts and zero-valent iron a likely source of natural abiotic nitrate remediation; added to their ranks now is the activity of iron-bearing phyllosilicate minerals.

## APPENDIX A

## TABLES

**Table 1.** Absorption Coefficients of Standards

| Standard Mass (g) | Dilution (L) | [Fe] (mol/L) | Fe(II) ε ($M^{-1}cm^{-1}$) | Total Fe ε ($M^{-1}cm^{-1}$) |
|---|---|---|---|---|
| 0.008 | 85.792 | 0.00023 | 934 | 1066 |
| 0.025 | 85.197 | 0.00074 | 964 | 1038 |
| 0.038 | 86.429 | 0.00112 | 939 | 1002 |
| 0.006 | 84.079 | 0.00018 | 929 | 1121 |
| 0.021 | 83.569 | 0.00064 | 936 | 1015 |
| 0.035 | 84.610 | 0.00105 | 958 | 1023 |
| 0.007 | 83.563 | 0.00021 | 953 | 1142 |
| 0.026 | 84.487 | 0.00078 | 960 | 1043 |
| 0.043 | 84.960 | 0.00129 | 952 | 1023 |
| 0.007 | 83.820 | 0.00021 | 1465* | 1679* |
| 0.018 | 83.702 | 0.00055 | 960 | 1072 |
| 0.032 | 83.342 | 0.00098 | 977 | 1076 |
| 0.007 | 80.916 | 0.00022 | 825 | 993 |
| 0.023 | 83.123 | 0.00071 | 990 | 1047 |
| 0.034 | 79.773 | 0.00109 | 975 | 1016 |
| 0.007 | 82.722 | 0.00022 | 809 | 1068 |
| 0.021 | 82.718 | 0.00065 | 934 | 1028 |
| 0.036 | 81.875 | 0.00112 | 920 | 1010 |
| 0.010 | 85.157 | 0.00031 | 843 | 1048 |
| 0.024 | 84.101 | 0.00073 | 920 | 1043 |
| 0.039 | 83.836 | 0.00119 | 938 | 1014 |
| | | Average | 931 | 1044 |
| | | Standard Deviation | 49 | 38 |

*Outliers. Not included in averages or standard deviations

**Table 2.** Variable Reduction Time Experiment Iron Analysis Results

| | Before Nitrate Treatment | | | After Nitrate Treatment | | |
|---|---|---|---|---|---|---|
| Reduction Time | mmol Fe(II) / g Clay | mmol Fe / g Clay | Fe(II)/Fe | mmol Fe(II) / g Clay | mmol Fe / g Clay | Fe(II)/Fe |
| Unaltered | 0.01 | 2.68 | 0.00 | 0.01 | 1.49 | 0.01 |
| 10 mins | 0.42 | 1.63 | 0.25 | 0.33 | 1.53 | 0.21 |
| 30 mins | 0.98 | 1.63 | 0.60 | 0.47 | 1.43 | 0.33 |
| 1 hr | 0.88 | 1.69 | 0.52 | 0.61 | 1.56 | 0.39 |
| 4 hr | 1.76 | 1.98 | 0.89 | 0.74 | 1.43 | 0.52 |

**Table 3.** Bacteria and AQDS Experiment Iron Analysis Results

| | | mmol Fe(II) / g Clay | mmol Fe / g Clay | Fe(II)/Fe |
|---|---|---|---|---|
| Before Nitrate Treatment | Bacteria | 0.05 | 0.86 | 0.06 |
| | Bacteria + AQDS | N.D. | N.D. | N.D. |
| | Dithionite | 0.63 | 1.25 | 0.50 |
| | Dithionite + AQDS | N.D. | N.D. | N.D. |
| After Nitrate Treatment | Bacteria | 0.02 | 0.69 | 0.03 |
| | Bacteria + AQDS | 0.01 | 0.69 | 0.02 |
| | Dithionite | 0.03 | 0.57 | 0.06 |
| | Dithionite +AQDS | 0.08 | 1.04 | 0.08 |

**Table 4.** Variable Reduction Time Experiment Nitrogen Speciation

| Sample | $[NO_x^-]$ (μM) | $[NO_2^-]$ (μM) | $[NH_4^+]$ (μM) |
|---|---|---|---|
| Unaltered #1 | 86.8 | 0.0 | 6.0 |
| Unaltered #2 | 87.3 | 0.0 | 2.9 |
| Unaltered #3 | 86.0 | 0.0 | 0.0 |
| 10 min #1 | 88.1 | 0.0 | 3.9 |
| 10 min #2 | 86.0 | 0.3 | 0.0 |
| 10 min #3 | 87.0 | 0.1 | 3.0 |
| 30 min #1 | 84.9 | 0.1 | 1.7 |
| 30 min #2 | 84.9 | 0.1 | 0.0 |
| 30 min #3 | 84.4 | 0.1 | 0.5 |
| 1 hr #1 | 83.2 | 0.2 | 0.0 |
| 1 hr #2 | 81.3 | 0.3 | 0.3 |
| 1 hr #3 | 85.8 | 0.2 | 0.2 |
| 4 hr #1 | 83.0 | 0.0 | 0.0 |
| 4 hr #2 | 83.4 | 0.1 | 0.0 |
| 4 hr #3 | 82.6 | 0.1 | 1.4 |

**Table 5.** Nitrate Reduced in Variable Reduction Time Experiments

| Reduction Time | $[NO_3^-]$ Remaining (mM) | $[NO_2^-]$ Present (mM) | $NO_3^-$ Reduced (mmol) |
|---|---|---|---|
| Unaltered | 0.0867 | 0.0000 | $2.6 \times 10^{-5}$ |
| 10 min | 0.0870 | 0.0002 | $2.2 \times 10^{-5}$ |
| 30 min | 0.0848 | 0.0001 | $6.6 \times 10^{-5}$ |
| 1 hr | 0.0834 | 0.0002 | $9.6 \times 10^{-5}$ |
| 4 hr | 0.0830 | 0.0001 | $1.02 \times 10^{-4}$ |

**Table 6.** Bacteria and AQDS Experiment Nitrogen Speciation

| Reduction Method | $[NO_3^-]$ (μM) | $[NO_2^-]$ (μM) | $[NH_4^+]$ (μM) |
|---|---|---|---|
| Dithionite | 19.7 | 1.8 | 7.9 |
| Dithionite + AQDS | 23.4 | 1.0 | 5.6 |
| Bacteria | 50.0 | 1.0 | 185.1 |
| Bacteria + AQDS | 21.1 | 16.2 | 226.6 |

## APPENDIX B

## FIGURES

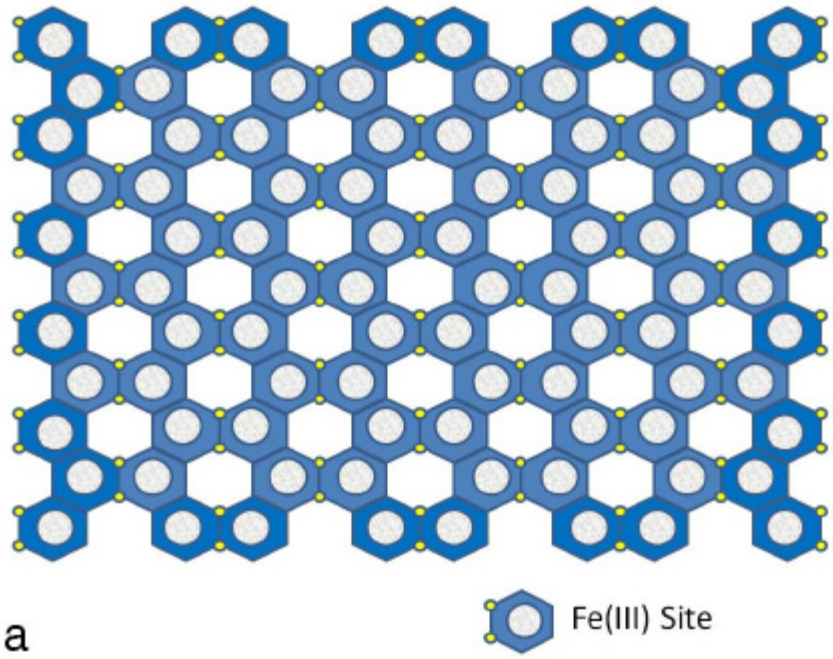


**Figure 1.** Theoretical occupancy of octahedral sites in an unaltered clay mineral. From Ribeiro et al (2009)

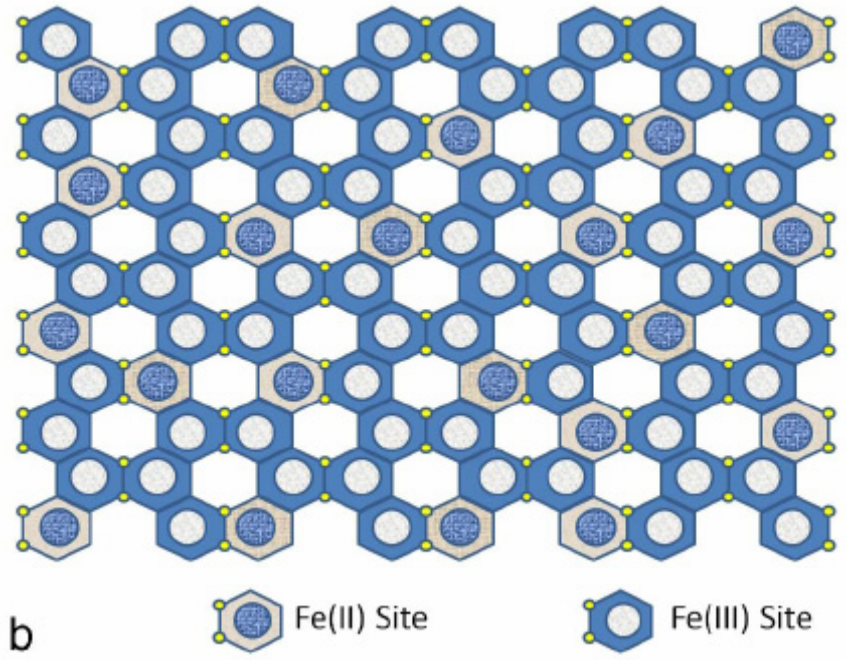


**Figure 2.** Theoretical occupancy of octahedral sites in a clay mineral after mild chemical reduction. Reduction occurs randomly along the basal surfaces. From Ribeiro et al (2009).

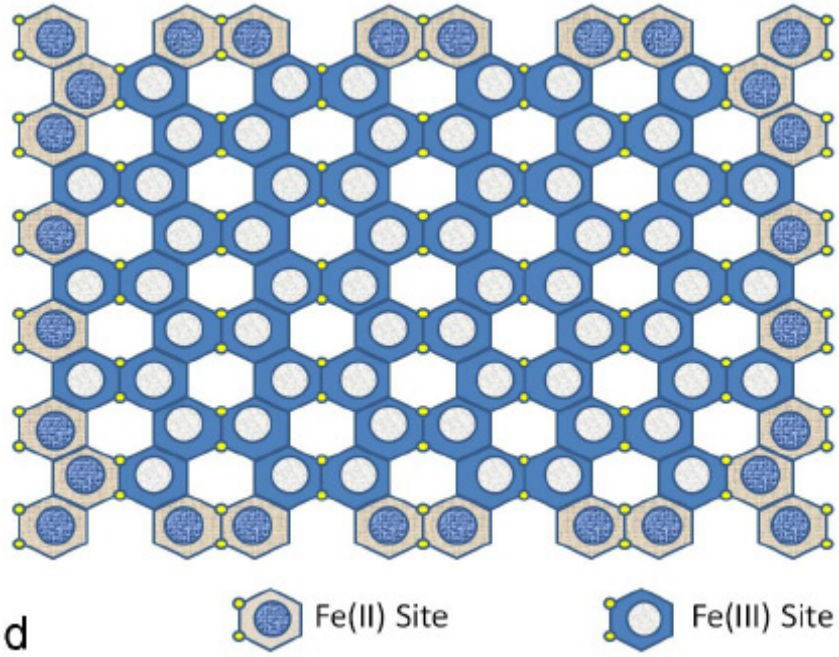


**Figure 3.** Theoretical occupancy of octahedral sites in a clay mineral after mild bacterial reduction. Edge sites, not the basal surfaces, are reduced. From Ribeiro et al (2009).

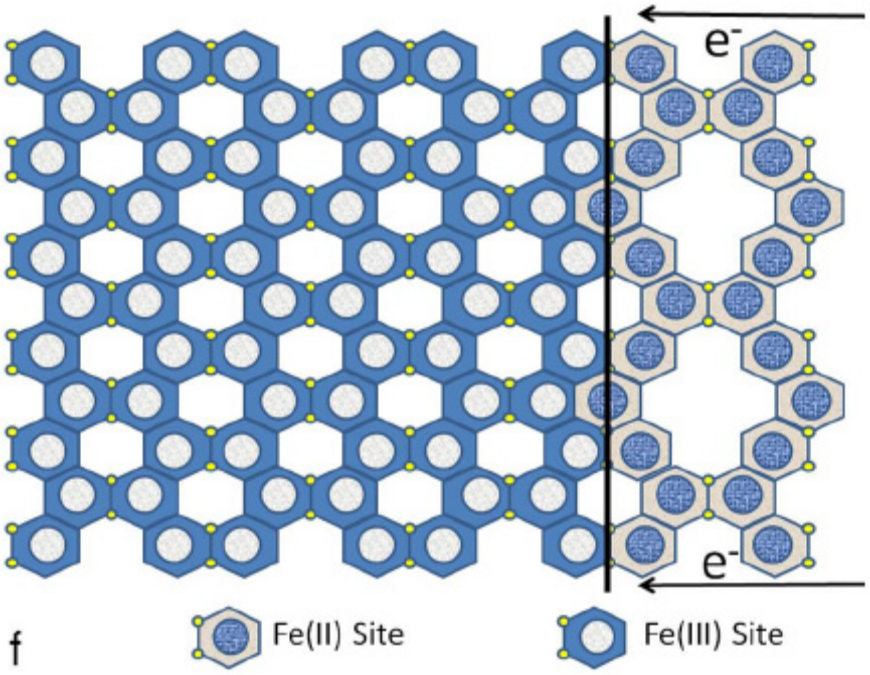


**Figure 4.** Theoretical occupancy of octahedral sites in a clay mineral after further bacterial reduction. Reduction front moves inward from edge sites. From Ribeiro et al (2009).

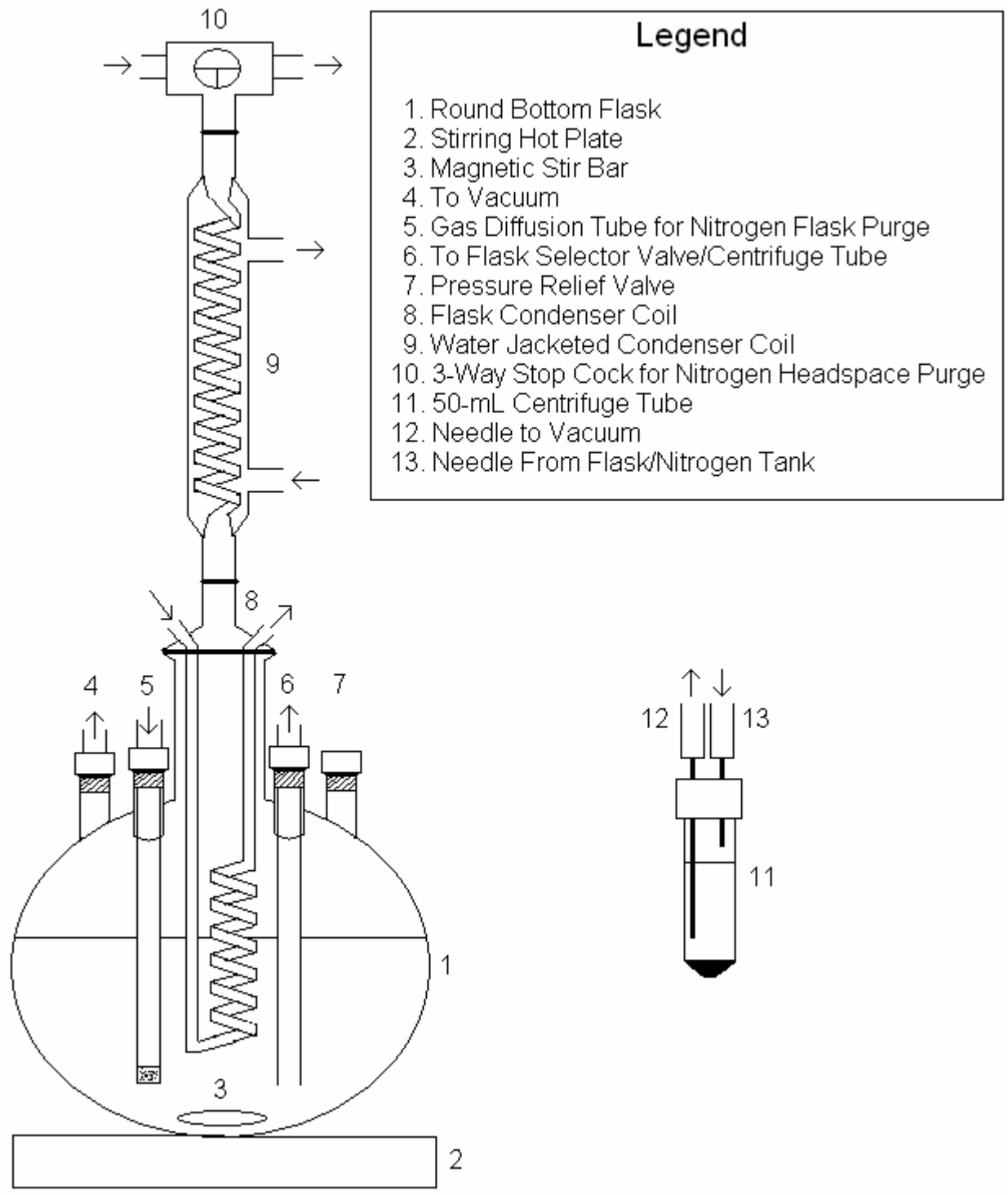


**Figure 5.** Diagram of washing apparatus

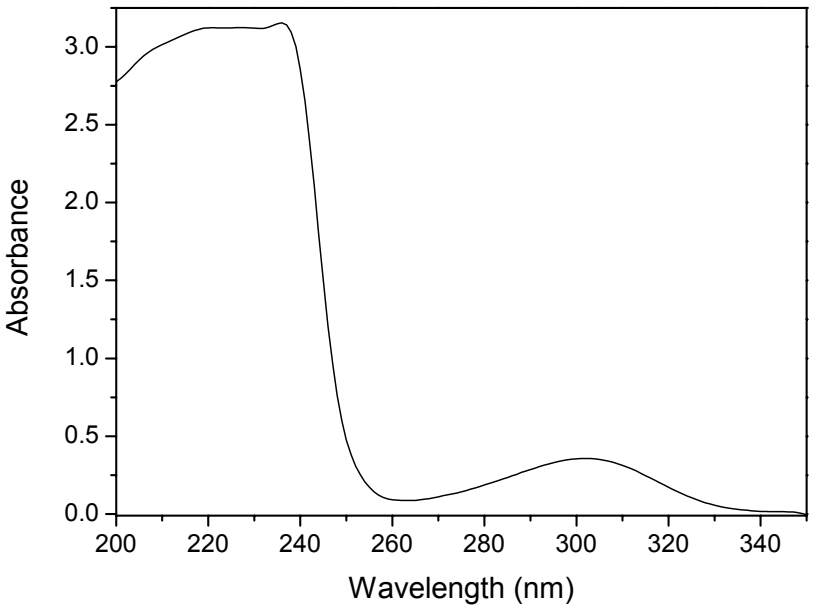


**Figure 6.** Absorption spectrum of 0.50 mM nitrate. Band at 300 nm is usable in this concentration range. The 200 nm band is stretched and absorbance values are much greater than 1.0.

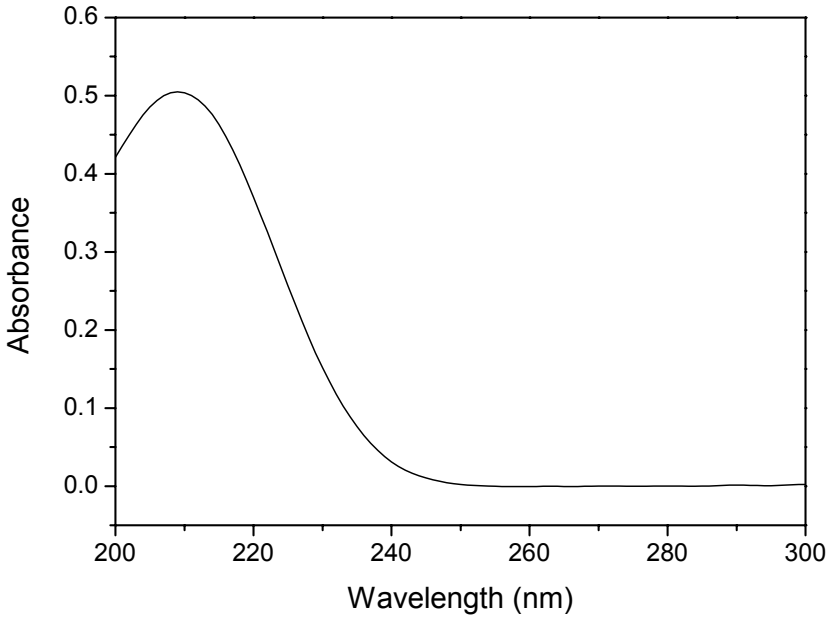


**Figure 7.** Absorption spectrum of 0.08 mM nitrite. Peak maximum is at 210 nm.

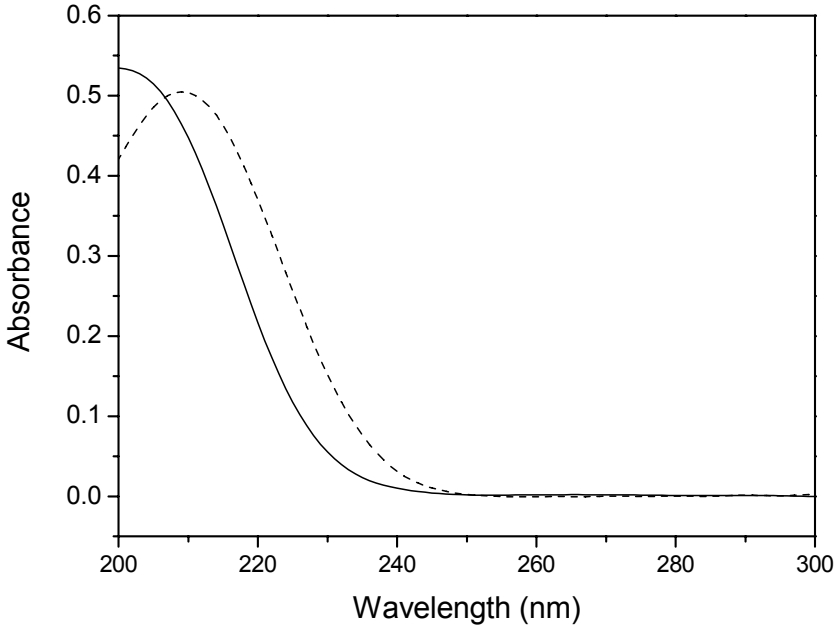


**Figure 8.** Absorption spectrum of 0.08 mM nitrite (solid) and 0.08 mM nitrate (dash). Nitrate peak occurs at 210 nm and no band appears at 300 nm at such dilute concentrations.

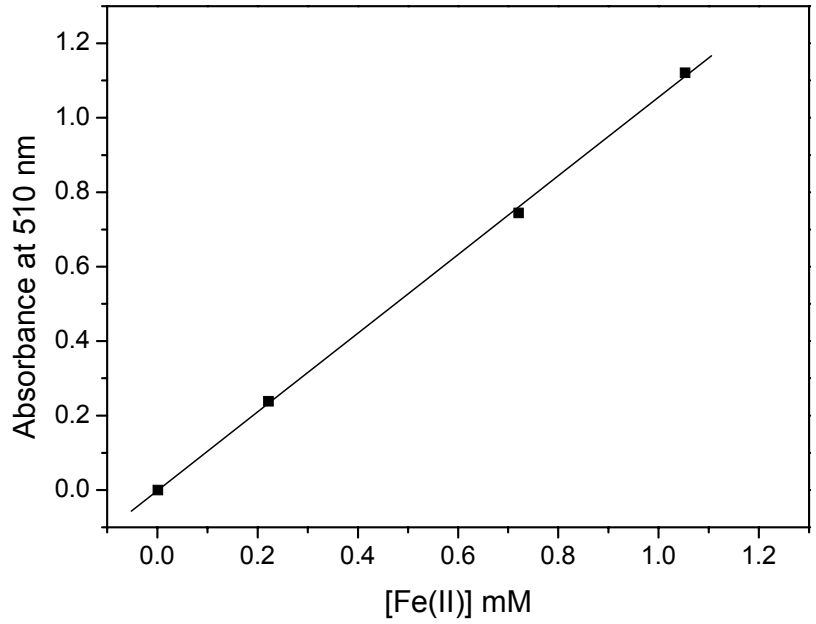


**Figure 9.** Sample calibration curve for Fe(II) analysis. $R^2 = 0.99974$.

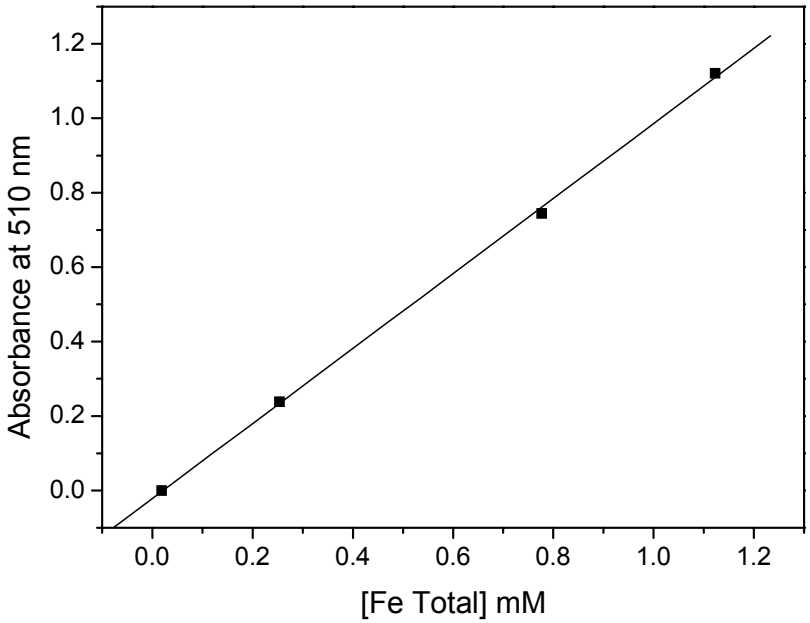


**Figure 10.** Sample calibration curve for total Fe. $R^2 = 0.99971$.

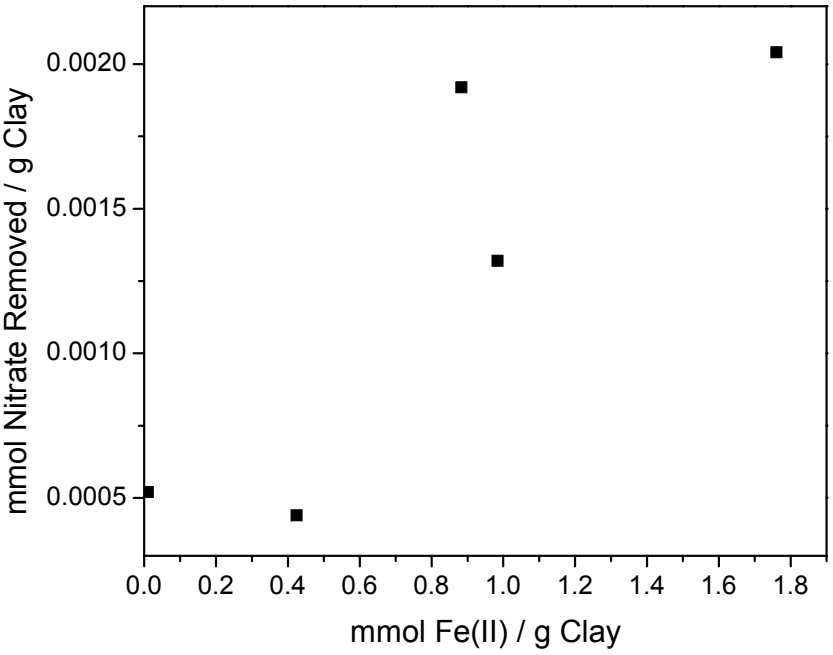


**Figure 11.** Plot showing the effect of the extent of reduction of a clay mineral on the amount of nitrate reduced. Variable Reduction time experiment only.

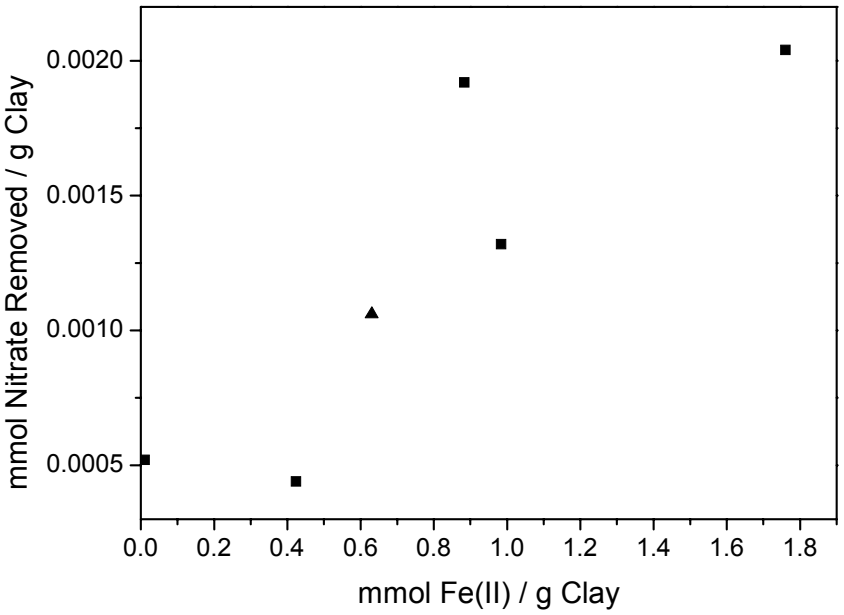


**Figure 12.** Plot showing the effect of the extent of reduction of a clay mineral on the amount of nitrate reduced. ■Variable reduction time experiments ▲Dithionite from bacteria and AQDS experiments.

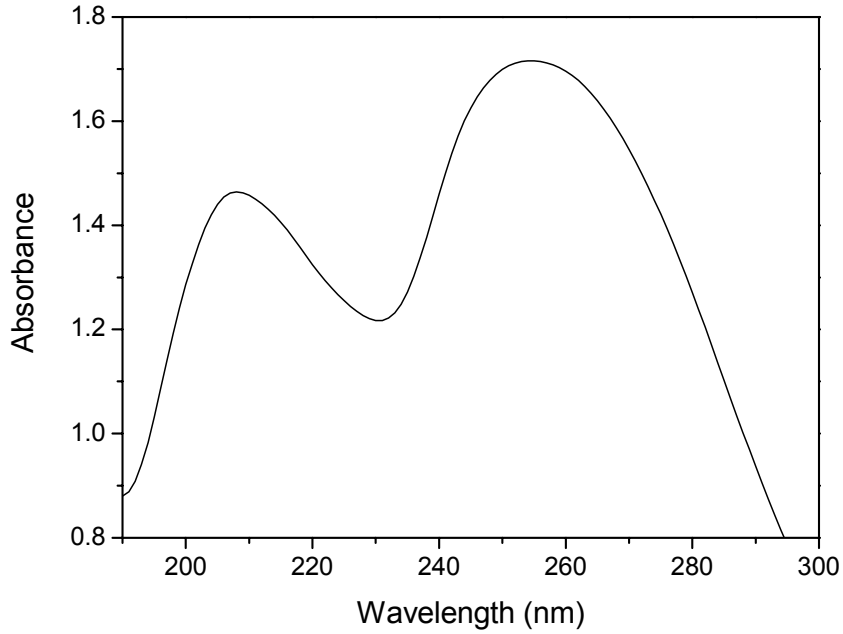


**Figure 13.** Initial absorbance spectrum of dithionite reduced clay with AQDS in a dilute nitrate solution within the flow reactor.

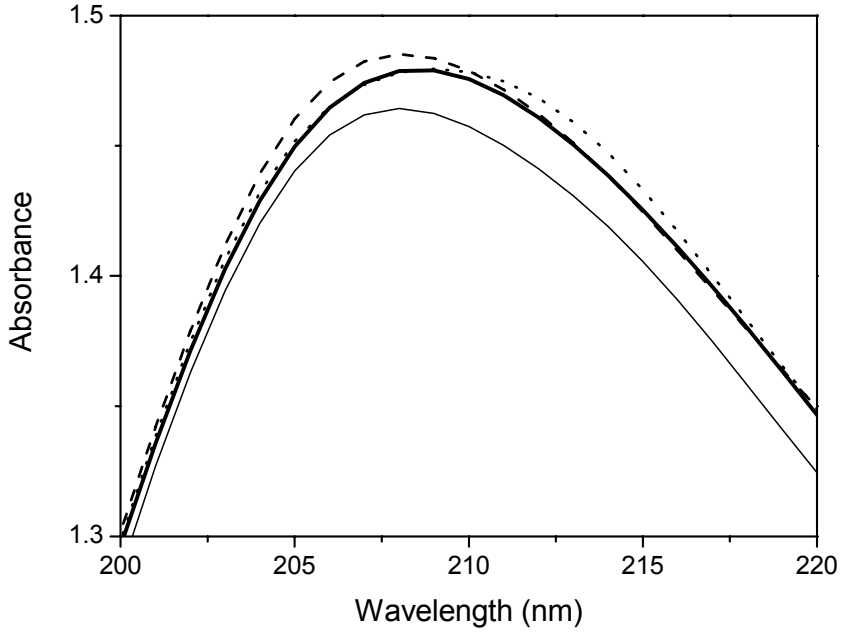


**Figure 14.** Dithionite and AQDS flow reactor experiment nitrate peak over time. Thin line for initial, dashed line for 4 hours, dotted line for 8 hours and thick line for 12 hours.

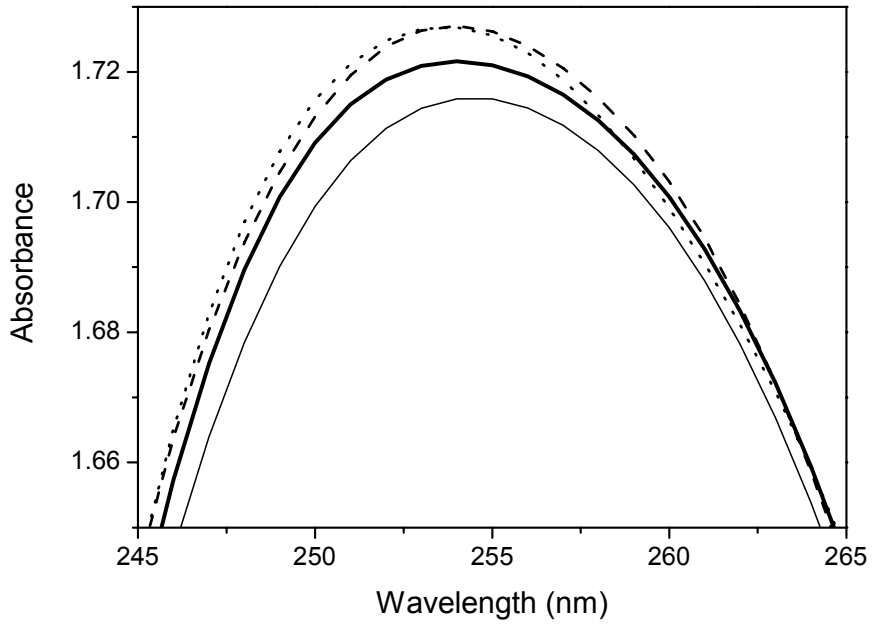


**Figure 15.** Dithionite and AQDS flow reactor experiment ferric-oxygen charge transfer band. Thin line for initial, dashed line for 4 hours, dotted line for 8 hours and thick line for 12 hours.

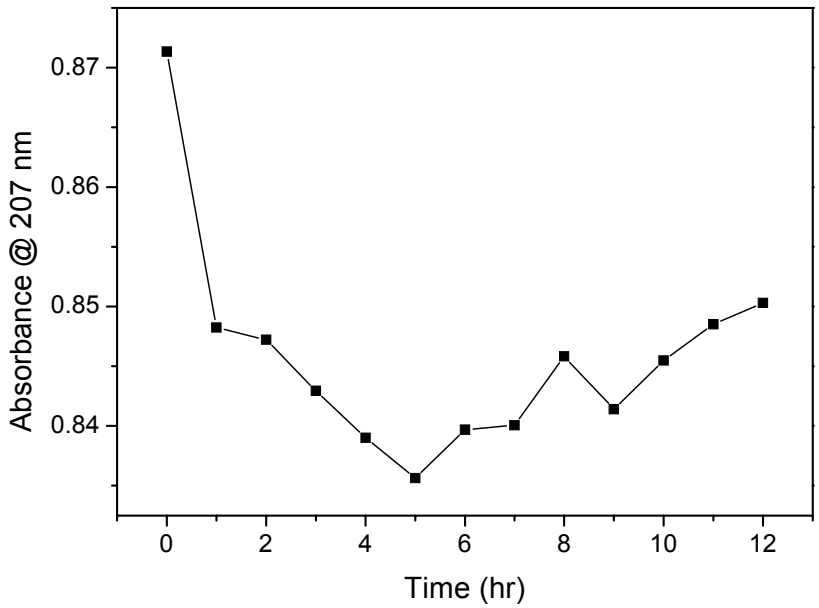


**Figure 16.** Separated nitrate peak values for dithionite with AQDS flow reactor experiment.

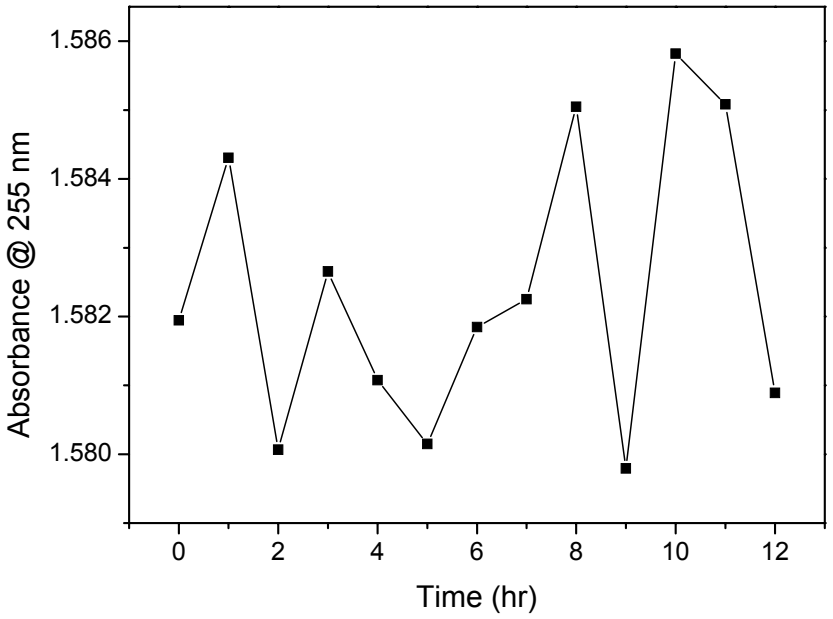


**Figure 17.** Separated ferric-oxygen charge transfer values for dithionite with AQDS flow reactor experiment.

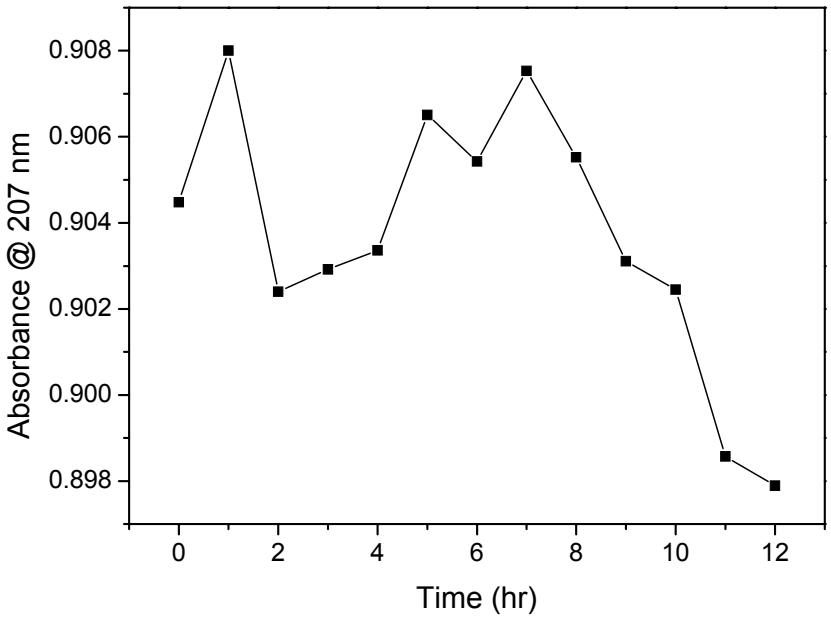


**Figure 18.** Separated nitrate peak values for bacteria flow reactor experiment.

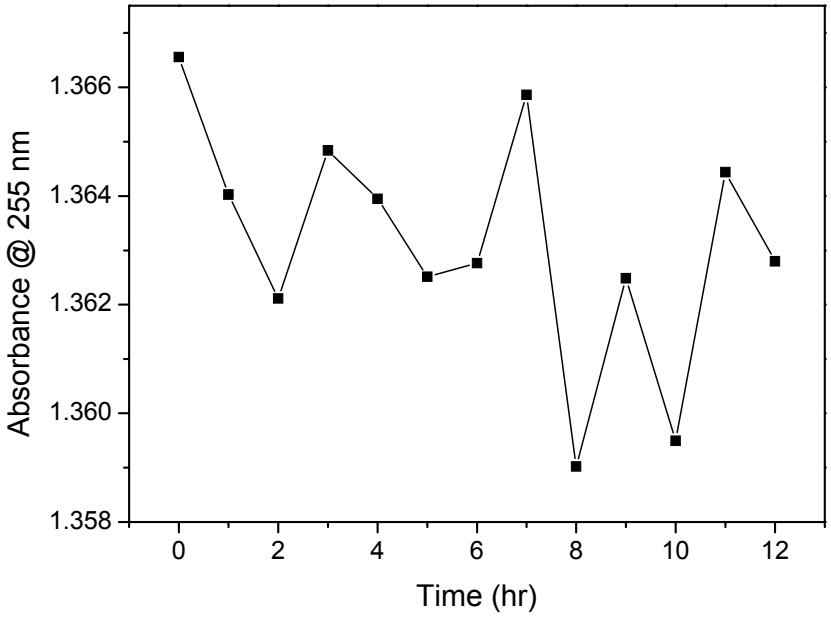


**Figure 19.** Separated ferric-oxygen charge transfer values for bacteria flow reactor experiment.

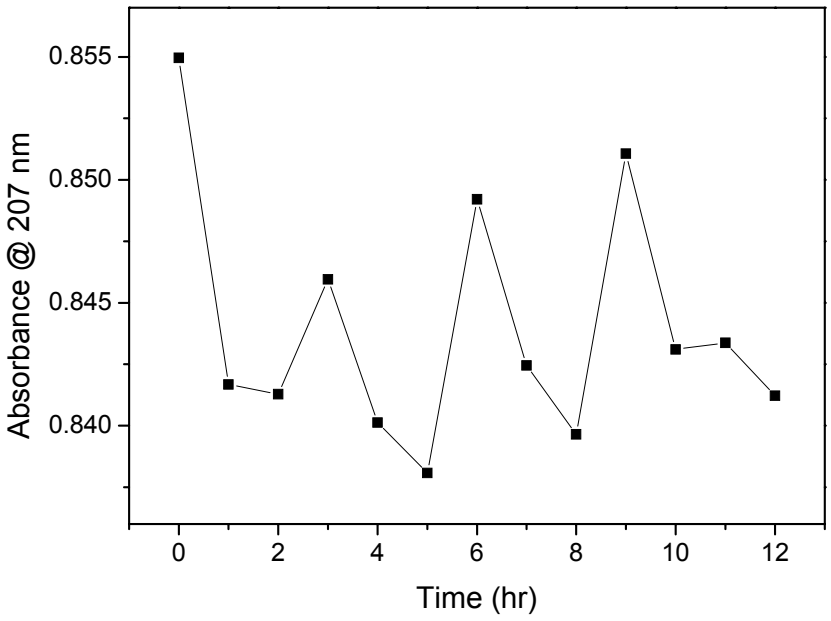


**Figure 20.** Separated nitrate peak values for bacteria with AQDS flow reactor experiment.

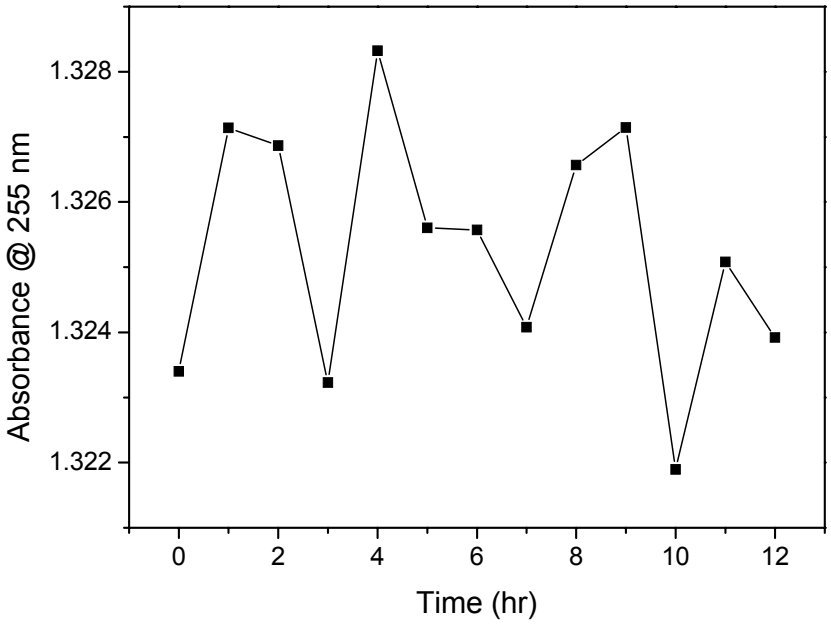


**Figure 21.** Separated ferric-oxygen charge transfer values for bacteria with AQDS flow reactor experiment.

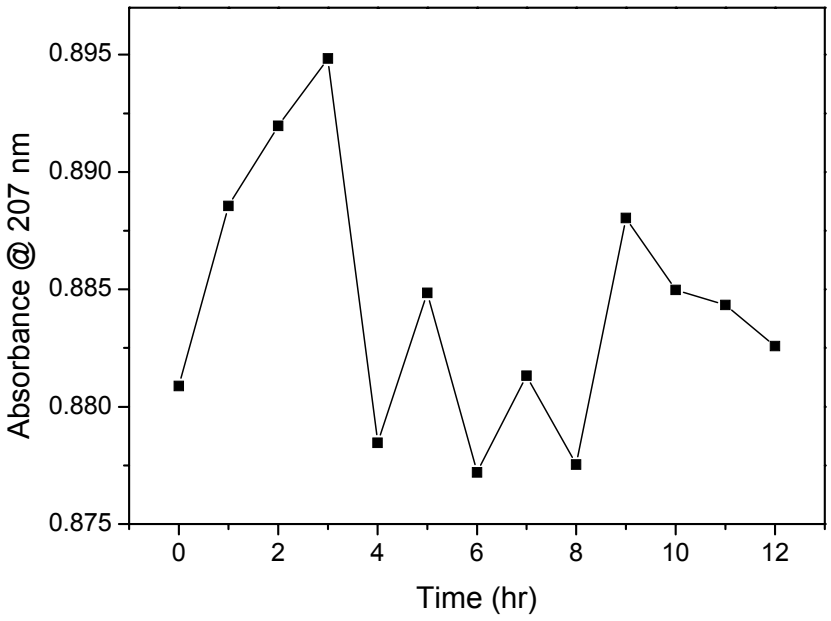


**Figure 22.** Separated nitrate peak values for deoxygenated zero-valent iron and clay flow reactor experiment.

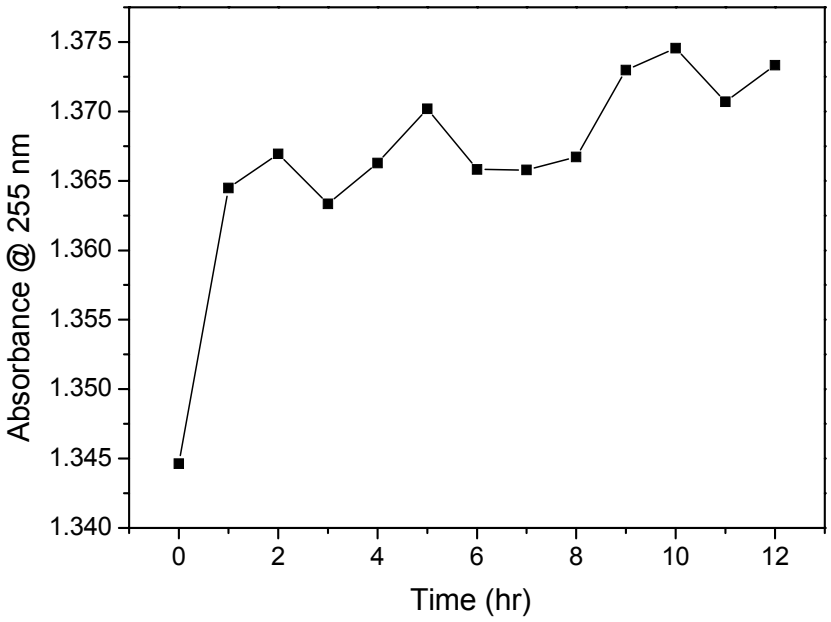


**Figure 23.** Separated ferric-oxygen charge transfer values for deoxygenated zero-valent iron and clay flow reactor experiment.

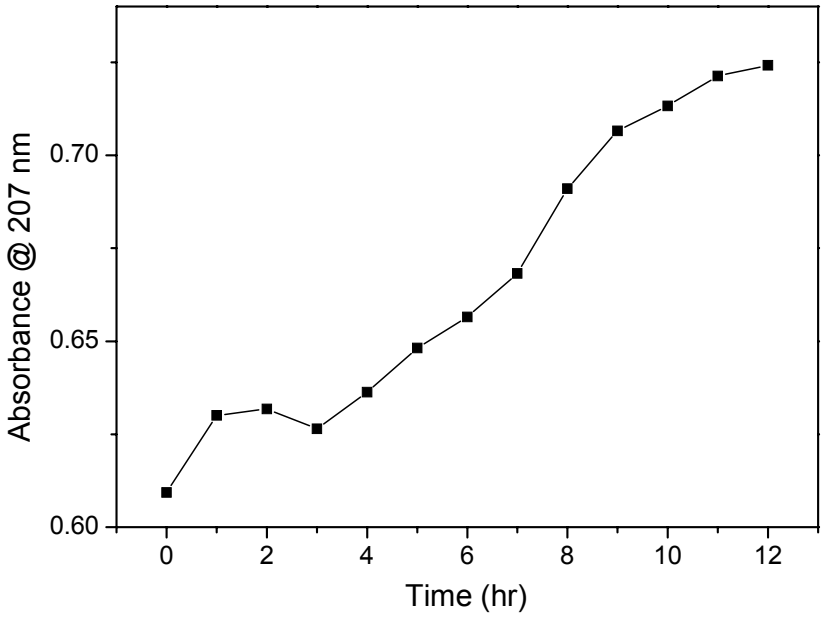


**Figure 24.** Separated nitrate peak values for oxygenated zero-valent iron and clay flow reactor experiment.

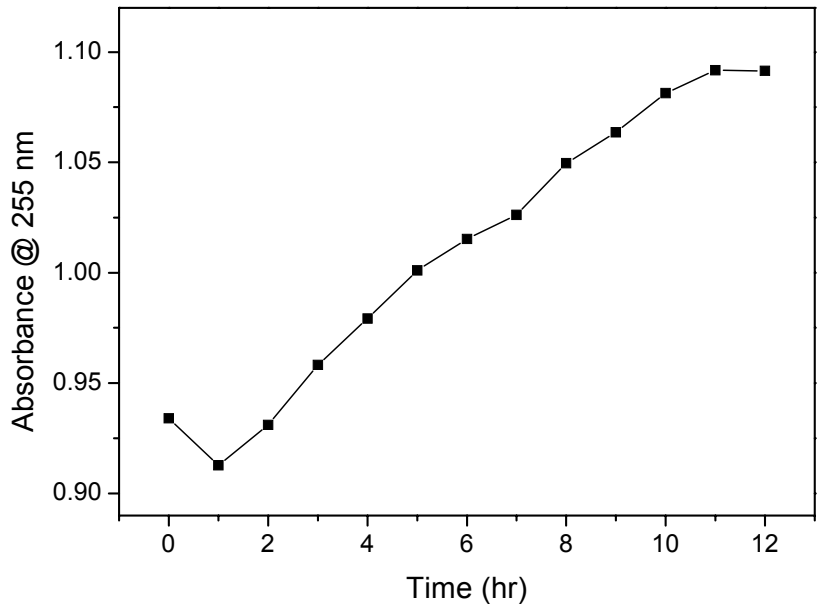


**Figure 25.** Separated ferric-oxygen charge transfer values for oxygenated zero-valent iron and clay flow reactor experiment.

## APPENDIX C

## LITERATURE CITED


Akob, D.M., Mills, H.J., Gihring, T.M., Kerkhof, L., Stucki, J.W., Anastácio, A.S., Chin, K-J., Küsel, K., Palumbo, A.V., Watson, D.B, Kostka., J.E. 2008. Enumeration, phylogenetic composition, and metabolic activity of nitrate- and Fe(III)-reducing bacteria catalyzing electron flow in radionuclide contaminated subsurface sediments. Applied and Environmental Microbiology, 74, 3159-3170.

Alowitz, M.J. & Scherer, M.M. 2002. Kinetics of nitrate, nitrite, and Cr(VI) reduction by iron metal. Environmental Science and Technology, 36, 299-306.

Aranda-Tamaura, C., Estrada-Alvarado, M.I., Texier, A., Cuervo, F. Gómez, J., Cervantes, F.J. 2007. Effects of different quinoid redox mediators on the removal of sulphide and nitrate via denitrification. Chemosphere, 69, 1722-1727.

Borch, T., Inskeep, W.P., Harwood, J.A., Gerlach, R. 2005. Impact of Ferrihydrite and Anthraquinone-2,6-Disulfonate on the Reductive Transformation of 2,4,6-Trinitrotoluene by a Gram-Positive Fermenting Bacterium. Environmental Science and Technology, 39, 7126-7133.

Bower, C.E. & Holm-Hansen, T. 1980. A Salicylate-Hypochlorite Method for Determining Ammonia in Seawater. Canadian Journal of Fisheries and Aquatic Sciences, 37, 794-798.

Braman, R.S. & Hendrix, S.A. 1989. Nanogram Nitrite and Nitrate Determination in Environmental and Biological Materials by Vanadium(III) Reduction with Chemiluminescence Detection. Analytical Chemistry, 61, 2715-2718.

Camargo, J.A. & Alonso, Á. 2006. Ecological and toxicological effects of inorganic nitrogen pollution in aquatic ecosystems: A global assessment. Environment International, 32, 831-849.

Cervantes, F.J., Gutierrez, C.H., Lopez, K.Y., Estrada-Alvarado, M.I., Meza-Escalante, E.R., Texier, A., Cuervo, F., Gómez, J. 2008. Contribution of quinone-reducing microorganisms to the anaerobic biodegradation of organic compounds u.nder different redox conditions. Biodegradation, 19, 235-246

Cervini-Silva, J., Wu, J., Stucki, J.W., Larson, R.A. 2000. Adsorption kinetics of pentachloroethane in iron-bearing smectites. Clays and Clay Minerals, 48, 132–138.

Cervini-Silva, J., Kostka, J.E., Larson, R.A., Stucki, J.W., Wu, J. 2003. Dehydrochlorination of 1,1,1 tricholoroethane and pentachloroethane by microbially reduced ferruginous smectite. Environmental Toxicology and Chemistry, 22, 1046–1050.

Cervini-Silva, J., Larson, R.A., Wu, J., Stucki., J.W. 2001. Transformation of chlorinated aliphatic compounds by ferruginous smectite. Environmental Science and Technology, 35, 805–809.

Cervini-Silva, J., Larson, R.A., Wu, J., Stucki, J.W. 2002. Dechlorination of pentachlorethane by commercial Fe and ferruginous smectite. Chemosphere, 47, 971–976.Chen, S.Z., P.F. Low, and C.B. Roth. 1987. Relation between potassium fixation and the oxidation state of octahedral iron. Soil Science Society of America Journal, 51, 82–86.

Chen, S.Z., Low, P.F, Roth, C.B. 1987. Relation between potassium fixation and the oxidation state of octahedral iron. Soil Science Society of America Journal, 51, 82–86

Devlin, J.F., Eedy, R.; Butler, B.J., 2000. Effect of electron donor and granular iron on nitrate transformation rates in sediments from a municipal water supply aquifer. Journal of Contaminant Hydrology, 46, 81-97.
Ernstsen, V. 1996. Reduction of Nitrate by Fe2+ in Clay Minerals. Clays and Clay Minerals, 44, 599-608
Ernstsen, V., Gates, W.P., Stucki J.W. 1998. Microbial reduction of structural iron in clays A renewable source of reduction capacity. Journal of Environmental Quality, 27, 761–766.
Garside, C. 1982. A chemiluminescent technique for the determination of nanomolar concentrations of nitrate and nitrite in seawater. Marine Chemistry, 11, 159-167.
Gates, W.P., Jaunet, A-M., Tessier, D., Cole, M.A., Wilkinson, H.T., Stucki, J.W. 1998. Swelling and texture of iron-bearing smectites reduced by bacteria. Clays and Clay Minerals, 46, 487–497.
Gates, W.P., Wilkinson, H.T., Stucki, J.W. 1993. Swelling properties of microbially reduced ferruginous smectite. Clays and Clay Minerals, 41, 360–364.
Hansen, H.C.B. & Koch, C.B. 1998. Reduction of nitrate to ammonium by sulphate green rust: Activation energy and reaction mechanism. Clay Minerals, 33, 87-101
Hansen, H.C.B., Borggaard, O.K., Sorensen, J. 1994. Evaluation of the free energy of formation of Fe(II)-Fe(III) hydroxide-sulphate (green rust) and its reduction of nitrite. Geochimica et Cosmochimica Acta, 58, 2599-2608
Hansen, H.C.B., Koch, C.B., Nanckekrogh, H., Borggaard, O.K., Sorensen, J. 1996. Abiotic nitrate reduction to ammonium: Key role of green rust. Environmental Science and Technology, 30, 2053-2056.
Hansen, H.C.B., Guldberg, S., Erbs, M., Koch, C.B. 2001. Kinetics of nitrate reduction by green rusts - Effects of interlayer anion and Fe(II):Fe(III) ratio. Applied Clay Science, 18, 81-91.
Hofstetter, T.B., Schwarzenbach, R.P., Haderlein., S.B. 2003. Reactivity of Fe(II) species associated with clay minerals. Environmental Science and Technology, 37, 519–528.
Hofstetter, T.B., Neumann, A., Schwarzenbach, R.P. 2006. Reduction of nitroaromatic compounds by Fe(II) species associated with iron-rich smectites. Environmental Science and Technology, 40, 235-242.
Hofstetter, T.B., Neumann, A, Arnold, W.A., Hartenbach, A., Bolotin, J., Cramer, C. J., Schwarzenbach, R.P. 2008. Substituent effects on nitrogen isotope fractionation during abiotic reduction of nitroaromatic compounds. Environmental Science and Technology
Huang, C.P., Wang, H.W., Chiu, P.C. 1998. Nitrate reduction by metallic iron. Water Resources, 32, 2257-2264.
Khaled, E.M. & Stucki, J.W. 1991. Fe oxidation state effects on cation fixation in smectites. Soil Science Society of America Journal, 55, 550–554.
Kim, J., Dong, H., Seabaugh, J., Newell, S.W., Eberl, D.D. 2004. Role of microbes in the illite-to-smectite reaction. Science, 303, 830-832.
Kim, J., Furukawa, Y., Daulton, T.E., Lavoie, D., Newell, S.W. 2003. Characterization of microbially Fe(III) reduced nontronite: environmental cell-transmission electron microscopy study. Clays and Clay Minerals, 51, 382–389.
Komadel, P., Lear, P.R., Stucki, J.W. 1990. Reduction and reoxidation of nontronite: extent of reduction and reaction rate. Clays and Clay Minerals, 38, 203-208.

Komadel, P. & Stucki, J.W. 1988. Quantitative assay of minerals for Fe2+ and Fe3+ using 1,10-phenanthroline: III. A rapid photochemical method. Clays and Clay Minerals, 36, 379-381.

Komadel, P., Stucki, J.W., Wilkinson, H.T. 1987. Reduction of structural iron in smectites by microorganisms. Pp. 322–324 In E. Galan (ed.) The Sixth Meeting of the European Clay Groups. Madrid.

Kostka, J.E., Haefele, E., Viehweger, R., Stucki, J.W. 1999a. Respiration and dissolution of Fe(III)-containing clay minerals by bacteria. Environmental Science and Technology, 33, 3127–3133.

Kostka, J.E., Stucki, J.W., Nealson, K.H., Wu, J. 1996. Reduction of structural Fe(III) in smectite by a pure culture of the Fe-reducing bacterium Shewanella putrefaciens strain MR-1. Clays and Clay Minerals, 44, 522–529.

Kostka, J.E., Wu, J., Nealson, K.H., Stucki, J.W. 1999b. The impact of structural Fe(III) reduction by bacteria on the surface chemistry of smectite clay minerals. Geochimica et Cosmochimica Acta, 63, 3705–3713.

Kwon, M.J. & Finneran, K.T. 2008. Biotransformation products and mineralization potential for hexahydro-1,3,5-trinitro-1,3,5-triazine (RDX) in abiotic versus biological degradation pathways with anthraquinone-2,6-disulfonate (AQDS) and Geobacter metallireducens. Biodegradation, 19, 705-715

Lear, P.R. & Stucki, J.W. 1989. Effects of iron oxidation state on the specific surface area of nontronite. Clays and Clay Minerals, 37, 547-552.

Manceau, A., Lanson, B., Drits, V.A., Chateigner, D., Wu, J., Huo, D., Gates, W.P., Stucki, J.W. 2000. Oxidation-reduction mechanism of iron in dioctahedral smectites. 2. Structural chemistry of reduced Garfield nontronite. American Mineralogist, 85, 153–172.

Miehr, R., Tratnyek. M.M., Bandstra, J.Z., Scherer, M.M., Alowitz, M.J., Bylaska, E.J. 2004. Diversity of contaminant reduction reactions by zerovalent iron: role of the reductate. Environmental Science andTechnology, 38, 139-147.

Mississippi River/Gulf of Mexico Watershed Nutrient Task Force. 2007. Draft Gulf Hypoxia 2008 Action Plan

Mulvaney, R.L. 1996. Nitrogen-Inorganic forms. p. 1123-1200. In D.L Sparks (ed.) Methods of soil analysis. Part 3. SSSA Book Ser. 5. SSSA, Madison, WI.

Norman, R.J., Stucki, J.W. 1981. The determination of nitrate and nitrite in soil extracts by ultra violet spectrophotometry. Soil Science Society of America Journal, 45, 347-353.

Ottley, C.J., Davison, W., Edmunds, W.M. 1997. Chemical catalysis of nitrate reduction by iron(II). Geochimica et Cosmochimica Acta, 61, 1819-1928.

Ribeiro, F.R., Fabris, J.D., Kostka, J.E., Komadel, P., Stucki, J.W. 2009. Comparisons of structural iron reduction in smectites by bacteria and dithionite: II. A variable-temperature Mossbauer spectroscopic study of Garfield notronite. Pure and Applied Chemistry, 81, 1499-1509.

Schwarzenbach, R.P., Stierli, R., Lanz, K., Zeyer, J. 1990. Quinone and iron porphyrin mediated reduction of nitroaromatic compounds in homogeneous aqueous solution. Environmental Science and Technology, 24, 1566-1574.

Shen, S. & Stucki, J.W. 1994. Effects of iron oxidation state on the fate and behavior of potassium in soils. Pp. 173–185 In J.L. Havlin et al. (eds.) Soil testing: prospects for improving nutrient recommendations, SSSA Special Publication 40. Soil Science Society of America, Madison, Wisconsin.

Sianta, D.P., Schreier, C.G., Chou, C.S., Reinhard, M. 1996. Treatment of 1,2-dibromo-3 chloropropane and nitrate-contaminated water with zerovalent iron or hydrogen/palladium catalysts. Water Resources, 30, 2315-2322.
Sohn, K., Kang, S.W., Ahn, S., Woo, M., Yang, S.K. 2006. Fe(0) nanoparticles for nitrate reduction: Stability, reactivity, and transformation. Environmental Science and Technology, 40, 5514-5519.
Stucki, J.W. 1988. Iron in smectites. Pp. 625-675 In J.W. Stucki, B.A. Goodman, and U. Schwertmann (eds.) Iron in soils and clay minerals. D. Reidel, Dordrecht, The Netherlands.
Stucki, J.W. & Getty, P.J. 1986. Microbial reduction of iron in nontronite. Agronomy Abstracts, 1986, 279
Stucki, J.W., Golden, D.C., Roth, C.B. 1984a. Effects of reduction and reoxidation of 12 structural Fe on the surface charge and dissolution of dioctahedral smectites. Clays and Clay Minerals, 32, 350–356.
Stucki, J.W., Golden, D.C., Roth, C.B. 1984b. Preparation and handling of dithionite-reduced smectite suspensions. Clays and Clay Minerals, 32, 191–197.
Stucki, J.W., Komadel, P., Wilkinson, H.T. 1987. Microbial reduction of structural iron(III) in smectites. Soil Science Society of America Journal, 51, 1663–1665.
Stucki, J.W. & Kostka, J.E. 2006. Microbial reduction of iron in smectite. Compte Rendu Geoscience, 338, 468-475.
Stucki, J.W., Lee, K., Goodman, B.A., Kostka, J.E. 2007. Effects of in situ biostimulation on iron mineral speciation in a sub-surface soil. Geochimica et Cosmochimica Acta, 71, 835-843.
Stucki, J.W., Lee, K., Zhang, L., Larson, R.A. 2002. The effects of iron oxidation state on the surface and structural properties of smectites. Pure and Applied Chemistry, 74, 2079-2092.
Stucki, J.W., Low, P.F., Roth, C.B., Golden, D.C. 1984c. Effects of oxidation state of octahedral iron on clay swelling. Clays and Clay Minerals, 32, 357–362.
Stucki, J.W. & Tessier, D. 1991. Effects of iron oxidation state on the texture and structural order of Na-nontronite gels. Clays and Clay Minerals, 39,137–143.
Till, B.A., Weathers, L.I., Alverez, P.J.J. 1998. Fe(0)-supported autotrophic denitrification. Environmental Science and Technology, 32, 634-639.
Westerhoff, P. 2003. Reduction of nitrate, bromate and chlorate by zero valent iron (Fe0). Journal of Environmental Engineering, 129, 10-16
Wu, J., Low, P.F., Roth, C.B. 1989. Effects of octahedral iron reduction and swelling pressure on interlayer distances in Na-nontronite. Clays and Clay Minerals, 37, 211–218.
Wu, J., Roth, C.B., Low, P.F. 1988. Biological reduction of structural Fe in sodium nontronite. Soil Science Society of America Journal, 52, 295–296.
Yan, L. & Bailey, G.W. 2001. Sorption and Abiotic Redox Transformation of Nitrobenzene at the Smectite-Water Interface. Journal of Colloid and Interface Science. 241. 142-153.

## APPENDIX D

## ANCILLARY DATA

**Table D.1.** Iron Analysis Data for Unaltered Samples

| Centrifuge Tube Contents | Tube Mass (g) | Tube + Standard (g) | Fe Analysis Tube Empty (g) | Tube + Contents + Dilution (g) | Fe(II) Abs | Fe Total Abs |
|---|---|---|---|---|---|---|
| 0 ppm | 19.482 | - | 21.444 | 106.287 | 0.000<br>0.000 | 0.016<br>0.036 |
| 1 ppm | 19.585 | 19.595 | 21.816 | 106.973 | 0.259<br>0.256 | 0.321<br>0.319 |
| 3 ppm | 19.792 | 19.816 | 21.820 | 105.921 | 0.670<br>0.669 | 0.760<br>0.758 |
| 6 ppm | 18.936 | 18.975 | 21.607 | 105.443 | 1.113<br>1.113 | 1.201<br>1.205 |
| Unaltered #1 | - | - | 21.813 | 106.703 | 0.005<br>0.006 | 1.630<br>1.638 |
| Unaltered #2 | - | - | 21.812 | 104.806 | 0.005<br>0.006 | 1.684<br>1.736 |
| Unaltered #3 | - | - | 21.796 | 106.652 | 0.004<br>0.008 | 1.630<br>1.635 |

**Table D.2.** Iron Analysis Data for 30 min Samples – Used only for Standard Calibration

| Centrifuge Tube Contents | Tube Mass (g) | Tube + Standard (g) | Fe Analysis Tube Empty (g) | Tube + Contents + Dilution (g) | Fe(II) Abs | Fe Total Abs |
|---|---|---|---|---|---|---|
| 0 ppm | 19.417 | - | 21.621 | 105.712 | 0.001<br>0.002 | 0.015<br>0.013 |
| 1 ppm | 19.454 | 19.461 | 21.633 | 104.355 | 0.175<br>0.174 | 0.235<br>0.226 |
| 3 ppm | 19.616 | 19.637 | 21.637 | 104.355 | 0.604<br>0.604 | 0.663<br>0.668 |
| 5 ppm | 19.852 | 19.888 | 21.630 | 103.505 | 1.027<br>1.036 | 1.131<br>1.134 |
| 30 min #1 | - | - | 21.697 | 105.815 | 0.330<br>0.331 | 0.929<br>0.971 |
| 30 min #2 | - | - | 21.626 | 106.746 | 0.689<br>0.690 | 1.042<br>1.040 |
| 30 min #3 | - | - | 21.633 | 105.759 | 0.594<br>0.592 | 1.040<br>1.032 |

**Table D.3.** Iron Analysis Data for 10 min and 30 min Samples

| Centrifuge Tube Contents | Tube Mass (g) | Tube + Standard (g) | Fe Analysis Tube Empty (g) | Tube + Contents + Dilution (g) | Fe(II) Abs | Fe Total Abs |
|---|---|---|---|---|---|---|
| 0 ppm | 19.457 | - | 21.443 | 107.983 | 0.001<br>0.001 | 0.020<br>0.018 |
| 1 ppm | 19.541 | 19.549 | 21.615 | 107.407 | 0.220<br>0.222 | 0.253<br>0.254 |
| 3 ppm | 19.058 | 19.083 | 21.636 | 106.833 | 0.721<br>0.722 | 0.777<br>0.777 |
| 5 ppm | 19.807 | 19.845 | 21.617 | 108.046 | 1.053<br>1.053 | 1.117<br>1.129 |
| 10 min #1 | - | - | 21.628 | 108.626 | 0.345<br>0.353 | 1.165<br>1.172 |
| 10 min #2 | - | - | 21.607 | 107.443 | 0.126<br>0.130 | 0.818<br>0.823 |
| 10 min #3 | - | - | 21.806 | 107.308 | 0.209<br>0.209 | 0.979<br>0.971 |
| 30 min #1 | - | - | 21.812 | 106.105 | 0.330<br>0.331 | 0.979<br>0.971 |
| 30 min #2 | - | - | 21.614 | 106.348 | 0.689<br>0.690 | 1.041<br>1.040 |
| 30 min #3 | - | - | 21.613 | 107.549 | 0.594<br>0.592 | 1.041<br>1.032 |

**Table D.4.** Iron Analysis Data for 1 hr Samples

| Centrifuge Tube Contents | Tube Mass (g) | Tube + Standard (g) | Fe Analysis Tube Empty (g) | Tube + Contents + Dilution (g) | Fe(II) Abs | Fe Total Abs |
|---|---|---|---|---|---|---|
| 0 ppm | 19.245 | - | 21.615 | 105.712 | 0.000<br>0.000 | 0.012<br>0.016 |
| 1 ppm | 19.754 | 19.761 | 21.232 | 104.795 | 0.204<br>0.203 | 0.245<br>0.243 |
| 3 ppm | 19.396 | 19.422 | 21.625 | 106.112 | 0.755<br>0.752 | 0.819<br>0.818 |
| 5 ppm | 19.546 | 19.589 | 21.816 | 106.776 | 1.230<br>1.227 | 1.321<br>1.319 |
| 1 hr #1 | - | - | 21.845 | 107.429 | 0.478<br>0.503 | 0.982<br>1.034 |
| 1 hr #2 | - | - | 21.811 | 106.818 | 0.342<br>0.344 | 0.836<br>0.844 |
| 1 hr #3 | - | - | 21.802 | 105.827 | 0.617<br>0.623 | 1.266<br>1.281 |

**Table D.5.** Iron Analysis Data for 4 hr Samples

| Centrifuge Tube Contents | Tube Mass (g) | Tube + Standard (g) | Fe Analysis Tube Empty (g) | Tube + Contents + Dilution (g) | Fe(II) Abs | Fe Total Abs |
|---|---|---|---|---|---|---|
| 0 ppm | 19.469 | - | 21.615 | 106.461 | 0.003<br>0.001 | 0.012<br>0.011 |
| 1 ppm | 19.554 | 19.560 | 21.615 | 105.694 | 0.169<br>0.169 | 0.205<br>0.203 |
| 3 ppm | 19.065 | 19.086 | 21.609 | 105.178 | 0.599<br>0.601 | 0.647<br>0.654 |
| 5 ppm | 19.820 | 19.855 | 21.813 | 106.423 | 1.008<br>1.014 | 1.074<br>1.085 |
| 4 hr #1 | - | - | 21.631 | 107.375 | 0.764<br>0.767 | 1.091<br>1.100 |
| 4 hr #2 | - | - | 21.617 | 106.112 | 1.037<br>1.037 | 1.219<br>1.226 |
| 4 hr #3 | - | - | 21.620 | 106.737 | 1.065<br>1.116 | 1.296<br>1.362 |

**Table D.6.** Iron Analysis Data for 1 hr and 4 hr Samples After Nitrate Reaction

| Centrifuge Tube Contents | Tube Mass (g) | Tube + Standard (g) | Fe Analysis Tube Empty (g) | Tube + Contents + Dilution (g) | Fe(II) Abs | Fe Total Abs |
|---|---|---|---|---|---|---|
| 0 ppm | 19.507 | - | 21.632 | 103.825 | 0.000<br>0.003 | 0.016<br>0.028 |
| 1 ppm | 19.880 | 19.887 | 21.815 | 105.635 | 0.311<br>0.313 | 0.357<br>0.358 |
| 3 ppm | 19.852 | 19.870 | 21.831 | 105.533 | 0.527<br>0.526 | 0.589<br>0.589 |
| 5 ppm | 19.828 | 19.860 | 21.631 | 104.973 | 0.957<br>0.957 | 1.006<br>1.014 |
| 1 hr #1 | - | - | 21.637 | 107.663 | 0.359<br>0.360 | 0.954<br>0.964 |
| 1 hr #2 | - | - | 21.628 | 108.283 | 0.300<br>0.301 | 0.901<br>0.904 |
| 1 hr #3 | - | - | 21.821 | 110.168 | 0.318<br>0.317 | 0.953<br>0.952 |
| 4 hr #1 | - | - | 21.235 | 114.341 | 0.369<br>0.369 | 0.804<br>0.803 |
| 4 hr #2 | - | - | 21.617 | 111.658 | 0.333<br>0.332 | 0.727<br>0.726 |
| 4 hr #3 | - | - | 21.616 | 109.790 | 0.428<br>0.452 | 0.922<br>0.973 |

**Table D.7.** Iron Analysis Data for Unaltered, 10 min, and 30 min Samples after Nitrate Reaction

| Centrifuge Tube Contents | Tube Mass (g) | Tube + Standard (g) | Fe Analysis Tube Empty (g) | Tube + Contents + Dilution (g) | Fe(II) Abs | Fe Total Abs |
|---|---|---|---|---|---|---|
| 0 ppm | 19.430 | - | 21.620 | 102.449 | 0.002<br>0.004 | 0.022<br>0.022 |
| 1 ppm | 19.468 | 19.475 | 21.619 | 102.535 | 0.213<br>0.151 | 0.252<br>.0186 |
| 3 ppm | 19.254 | 19.277 | 21.624 | 104.747 | 0.702<br>0.695 | 0.743<br>0.735 |
| 5 ppm | 19.562 | 19.596 | 21.629 | 101.402 | 1.060<br>0.906 | 1.104<br>0.951 |
| Unaltered #1 | - | - | 21.624 | 108.816 | 0.007<br>0.005 | 0.945<br>0.941 |
| Unaltered #2 | - | - | 21.823 | 107.639 | 0.006<br>0.002 | 0.883<br>0.311 |
| Unaltered #3 | - | - | 21.812 | 107.242 | 0.003<br>0.006 | 0.887<br>0.892 |
| 10 min #1 | - | - | 21.617 | 110.645 | 0.147<br>0.151 | 0.837<br>0.848 |
| 10 min #2 | - | - | 21.632 | 108.938 | 0.253<br>0.260 | 0.994<br>1.007 |
| 10 min #3 | - | - | 21.818 | 109.951 | 0.118<br>0.120 | 0.869<br>0.876 |
| 30 min #1 | - | - | 21.633 | 110.758 | 0.236<br>0.235 | 0.801<br>0.800 |
| 30 min #2 | - | - | 21.633 | 110.168 | 0.210<br>0.210 | 0.820<br>0.819 |
| 30 min #3 | - | - | 21.645 | 105.748 | 0.293<br>0.310 | 0.918<br>0.970 |

**Table D.8.** Iron Analysis of Dithionite and Bacteria Reduced Samples Before Nitrate Reaction*

| Tube Contents | Empty Mass (g) | Tube + Sample (g) | Tube, Sample + Dilution (g) | Fe(II) Abs | Total Fe Abs |
|---|---|---|---|---|---|
| 0 ppm | 21.632 | - | 107.156 | 0.013<br>0.005 | 0.015 |
| 1 ppm | 21.808 | 21.816 | 107.882 | 0.256<br>0.254 | 0.300 |
| 4 ppm | 21.630 | 21.656 | 106.853 | 0.686<br>0.691 | 0.764 |
| 7 ppm | 21.832 | 21.889 | 106.641 | 0.0686<br>1.321 | 0.836 |
| 10 ppm | 21.819 | 21.890 | 107.286 | 0.756<br>1.294 | 0.946 |
| Dithionite | 21.614 | 21.637 | 108.014 | 0.337<br>0.343 | 0.757 |
| Bacteria | 21.819 | 21.850 | 106.785 | 0.056<br>0.060 | 1.107 |

*Standards not used in averages in Table 1

**Table D.9.** Iron Analysis of Dithionite and Bacteria Reduced Samples After Nitrate Reaction*

| Tube Contents | Empty Mass (g) | Tube + Sample (g) | Tube, Sample + Dilution | Fe(II) Abs | Total Fe Abs |
|---|---|---|---|---|---|
| 0 ppm | 21.632 | - | 106.723 | 0.000<br>0.001 | 0.011<br>0.015 |
| 1 ppm | 21.848 | 21.850 | 107.499 | 0.107<br>0.120 | 0.130<br>0.131 |
| 4 ppm | 21.834 | 21.847 | 107.058 | 0.355<br>0.356 | 0.395<br>0.395 |
| 7 ppm | 21.823 | 21.845 | 108.338 | 0.660<br>0.652 | 0.695<br>0.702 |
| 10 ppm | 21.806 | 21.836 | 107.366 | 0.839<br>0.842 | 0.871<br>0.878 |
| Bacteria | 21.629 | 21.656 | 108.199 | 0.025<br>0.027 | 0.865<br>0.870 |
| Dithionite | 21.814 | 21.824 | 108.879 | 0.016<br>0.019 | 0.340<br>0.341 |
| Dith + AQDS | 21.634 | 21.653 | 108.540 | 0.040<br>0.048 | 0.621<br>0.631 |
| Bact + AQDS | 21.819 | 21.846 | 109.435 | 0.016<br>0.016 | 0.857<br>0.859 |

* Standards not used in averages in Table 1

**Table D.10.** Nitrogen Analysis Results for Variable Time Reduction Experiments

| Sample | $NO_x^-$ (μm) | $NO_2^-$ (μm) | $NH_4^-$ (μm) |
|---|---|---|---|
| Unaltered #1 | 86.8 | 0.0 | 6.0 |
| Unaltered #2 | 87.3 | 0.0 | 2.9 |
| Unaltered #3 | 86.0 | 0.0 | 0.0 |
| 10 minutes #1 | 88.1 | 0.0 | 3.9 |
| 10 minutes #2 | 86.0 | 0.3 | 0.0 |
| 10 minutes #3 | 87.0 | 0.1 | 3.0 |
| 30 minutes #1 | 84.9 | 0.1 | 1.7 |
| 30 minutes #2 | 84.9 | 0.1 | 0.0 |
| 30 minutes #3 | 84.4 | 0.1 | 0.5 |
| 1 hour #1 | 83.2 | 0.2 | 0.0 |
| 1 hour #2 | 81.3 | 0.3 | 0.3 |
| 1 hour #3 | 85.8 | 0.2 | 0.2 |
| 4 hours #1 | 83.0 | 0.0 | 0.0 |
| 4 hours #2 | 83.4 | 0.1 | 0.0 |
| 4 hours #3 | 82.6 | 0.1 | 1.4 |

**Table D.11.** Nitrogen Analysis Results for Bacteria and AQDS Experiments

| Sample | $NO_x^-$ (μm) | $NO_2^-$ (μm) | $NH_4^-$ (μm) |
|---|---|---|---|
| Dithionite 1 | 18.7 | 2.2 | 10.5 |
| Dithionite 2 | 24.1 | 1.3 | 5.3 |
| Dithionite + AQDS 1 | 24.4 | 1.0 | 3.7 |
| Dithionite + AQDS 2 | 24.5 | 1.0 | 7.6 |
| Bacteria 1 | 70.9 | 1.2 | 130.6 |
| Bacteria 2 | 31.3 | 0.9 | 239.6 |
| Bacteria + AQDS 1 | 64.3 | 21.1 | 231.5 |
| Bacteria + AQDS 2 | 30.3 | 11.2 | 221.6 |